AMERICAN SOCIETY FOR MICROBIOLOGY | Applied and Environmental Microbiology

Genetics and Molecular Biology | Full-Length Text

Genetic dissection of the degradation pathways for the mycotoxin fusaric acid in *Burkholderia ambifaria* T16

Matias Vinacour,[1] Mauro Moiana,[1] Ignasi Forné,[2] Kirsten Jung,[3] Micaela Bertea,[1] Patricia M. Calero Valdayo,[4] Pablo I. Nikel,[4] Axel Imhof,[2] Miranda C. Palumbo,[5] Dario Fernández Do Porto,[5,6] Jimena A. Ruiz[1,3,4]

AUTHOR AFFILIATIONS See affiliation list on p. 19.

ABSTRACT Fusaric acid (FA) is a mycotoxin produced by several *Fusarium* species. *Burkholderia ambifaria* T16 is a rhizosphere bacterium, able to use FA as sole nitrogen, carbon, and energy source. By screening a transposon insertional library, combined with proteomic analysis, genes and enzymes involved in the microbial degradation of FA were identified for the first time. A functional 2-methylcitrate cycle, an anaplerotic pathway where propionyl-coenzyme A (CoA) is converted to pyruvate and succinate, was shown to be essential for growth in the presence of FA. The proteomic profile of *B. ambifaria* T16 showed that more than 50 enzymes (including those belonging to the 2-methylcitrate cycle, fatty acid metabolism, valine catabolism, and flavin biosynthesis) were significantly more abundant when growing on FA than on citrate. Flavin mononucleotide (FMN)-dependent luciferases like monooxygenase (LLM) are shown to catalyze the pyridine-ring cleavage reaction of several N-heterocyclic compounds. Deletion of a gene encoding a predicted LLM enzyme that was highly upregulated during growth on FA, completely abolished the capability of *B. ambifaria* T16 to grow with this mycotoxin as sole nitrogen, carbon, and energy source. Re-introduction of the wild type gene was able to restore growth. The mentioned gene is part of a gene cluster of unknown function that we termed *fua*, due to its probable role in fusaric acid catabolism. Our results suggest that the LLM encoded in the *fua* cluster catalyzes the pyridine-ring opening reaction during FA degradation, and that propionyl-CoA is one of the intermediates of FA catabolism in *B. ambifaria* T16.

IMPORTANCE Fusaric acid (FA) is an important virulence factor produced by several *Fusarium* species. These fungi are responsible for wilt and rot diseases in a diverse range of crops. FA is toxic for animals, humans and soil-borne microorganisms. This mycotoxin reduces the survival and competition abilities of bacterial species able to antagonize *Fusarium* spp., due to its negative effects on viability and the production of antibiotics effective against these fungi. FA biodegradation is not a common characteristic among bacteria, and the determinants of FA catabolism have not been identified so far in any microorganism. In this study, we identified genes, enzymes, and metabolic pathways involved in the degradation of FA in the soil bacterium *Burkholderia ambifaria* T16. Our results provide insights into the catabolism of a pyridine-derivative involved in plant pathogenesis by a rhizosphere bacterium.

KEYWORDS *Burkholderia ambifaria* T16, fusaric acid, two-component flavin-dependent monooxygenase, 2-methylcitrate cycle, detoxification, catabolism

Fusaric acid (FA, 5-butylpyridine-2-carboxylic acid) is a secondary metabolite synthesized by several *Fusarium* species (e.g., *F. oxysporum*, *F. solani*, *F. verticillioides*, *F. proliferatum*, and *F. subglutinans*) (1). These fungi are responsible for important wilt and rot diseases in a diverse range of crops, including maize, cucurbits, legumes,

Editor Arpita Bose, Washington University in St. Louis, Missouri, USA

Address correspondence to Jimena A. Ruiz, jruiz@agro.uba.ar.

The authors declare no conflict of interest.

See the funding table on p. 19.

Received 20 April 2023
Accepted 25 October 2023
Published 6 December 2023

tomato, onion, potato, and banana (2). Production of FA by different phytopathogenic *Fusarium* spp. has been evaluated *in vitro* and *in planta*. In most cases, a positive correlation between FA production and virulence was observed (3–8), which has led to the consideration of FA as one of the main virulence factors produced by *Fusarium* spp. FA has been described to possess several negative effects on plant cells, including reduction in the availability of metals (9), oxidative damage (5, 10, 11), loss of mitochondrial membrane potential (5, 12, 13), and a reduction in the content of photosynthetic pigments (11, 14).

Management of *Fusarium* wilt is mainly performed by crop rotation, cover cropping, soil disinfection, applying chemical fungicides, and cultivating-resistant varieties (15–18). However, several important crops do not possess *Fusarium* wilt-resistant varieties. Besides, the use of fungicides contributes to the development of new pathogen races that overcome host resistance, negatively impacting the environment.

One interesting and sustainable alternative to control *Fusarium* plant diseases is the use of biocontrol agents. However, FA is also harmful for soil-borne microorganisms (19). Gram-positive microorganisms (19–21) and mycobacteria (22) were shown to be highly sensitive to FA. Fluorescent pseudomonads, conversely, possess high tolerance to this mycotoxin (19, 21, 23). However, it was demonstrated that even low FA concentrations negatively affect growth rates (23), and the production of some antifungal metabolites implicated in the suppression of soil-borne fungal pathogens (24–27). These results highlight the important role of FA in the colonization of competitive environments by mycotoxigenic fungi (28), as this compound reduces the survival and competition abilities of soil microbes. In this context, the search of plant growth-promoting microorganisms able to detoxify FA, and the study of the mechanisms involved in mycotoxin detoxification, would greatly contribute to the design of novel biocontrol strategies. While fungi that are able to convert FA to less phytotoxic intermediates have been reported (29–31), the capability to catabolize FA seems to be much rare among soil-borne microorganisms. *Burkholderia ambifaria* T16 is a bacterial strain isolated from the rhizosphere of barley, able to use FA as the sole carbon, nitrogen, and energy source (32). When inoculated into barley seedlings exposed to FA, strain T16 was able to suppress the toxic effect of FA on the growth of roots and stems (32). In this study, we employed two different experimental approaches to explore FA catabolism in *B. ambifaria* T16. The construction of a mini-Tn*5* insertional library, combined with genome-wide proteome analyses, allowed us to identify genes, enzymes, and metabolic pathways that support bacterial growth on FA.

MATERIALS AND METHODS

Bacterial strains and culture conditions

Bacterial strains used in this work are listed in Table 1. *Escherichia coli* strains were routinely grown in LB medium under aeration at 37°C. *B. ambifaria* strains were cultivated at 32°C in LB medium or M9 minimal medium (33) supplemented with 1 mM $MgSO_4$, 0.1% (vol/vol) metal trace solution (34), and 0.2% (wt/vol) sodium citrate (M9 + CA), 0.2% (wt/vol) sodium propionate (M9 + PA) or 450 µg/mL FA (M9 +FA) as carbon sources. Solid media were prepared by adding 1.5% (wt/vol) agar. When needed, the following antibiotics were added to the culture medium: ampicillin (Amp) 100 µg/mL (*E. coli*), chloramphenicol (Cm) 34 µg/mL (*E. coli*), trimethoprim (Tmp) 10 µg/mL (*E. coli*) or 70 µg/mL (*B. ambifaria*), kanamycin (Km) 50 µg/mL (*E. coli*) or 400 µg/mL (*B. ambifaria*), gentamycin (Gm) 10 µg/mL (*E. coli*), tetracycline (Tc) 20 µg/mL (*E. coli*) or 200 µg/mL (*B. ambifaria*), and potassium tellurite (Tel) 20 µg/mL (*E. coli* and *B. ambifaria*).

To evaluate the growth of *B. ambifaria* strains with sodium citrate (CA) or sodium propionate (PA), an overnight culture in LB broth was inoculated at a 1/100 ratio into M9 + CA to prepare the inoculum. The inoculum for M9 + FA was prepared in M9 + CA supplemented with 90 µg/mL FA. After overnight growth, cells were centrifuged, washed two times with M9 without carbon source, and resuspended in 1 mL of the same

TABLE 1 Bacterial strains, plasmids, and oligonucleotides

Strain, plasmid, or oligonucleotide	Relevant genotype or description	Reference or source
Bacterial strains		
Escherichia coli		
CC118 *λpir*	Cloning host; Δ(*ara-leu*) *araD ΔlacX174 galE galK phoA thiE1 rpsE rpoB* (Rif^r) *argE* (Am) *recA1*; *λpir* lysogen	(35)
DH5α *λpir*	Cloning host; F$^-$*endA1 glnV44 thi-1 recA1 relA1 gyrA96 deoR nupG* Φ80d*lacZ*ΔM15 Δ(*lacZYA-argF*) U169; *hsdR17*(r_K^- m_K^+)/*λpir*	(36)
HB101	Helper strain; F$^-$λ$^-$*hsdS20* (*rB*$^-$*mB*$^-$) *recA13 leuB6* (Am) *araC14* Δ(*gpt-proA*)62 l*acY1 galK2* (Oc) *xyl-5 mtl-1 thiE1*	(35)
Burkholderia ambifaria		
T16	Wild type; isolated from the rhizosphere of barley; Tc^r	(32)
FA2	Derived of T16; *prpB*::mini-Tn*5*Tel;Tc^r Tel^r	This work
FA3	Derived of T16; *mlaD*::mini-Tn*5*Tel; Tc^r Tel^r	This work
FA4	Derived of T16; *prpR*::mini-Tn*5*Tel; Tc^r Tel^r	This work
FA21	Derived of T16; EIB72_16280::mini-Tn*5*Tel;Tc^r Tel^r	This work
FA84	Derived of T16, EIB72_11905::mini-Tn*5*Tel; Tc^r Tel^r	This work
FA90	Derived of T16; EIB72_05180–85::mini-Tn*5*Tel; Tc^r Tel^r	This work
FA91	Derived of T16; *prpF*::mini-Tn*5*Tel; Tc^r Tel^r	This work
FA92	Derived of T16; *prpR*::mini-Tn*5*Tel; Tc^r Tel^r	This work
T42	Derived of T16; Δ*prpB*; Tc^r	This work
T800	Derived of T16; Δ*fuaC*; Tc^r	This work
Mycobacterium smegmatis mc^2 155	High-frequency transformation mutant of *M. smegmatis* ATCC 607	(37)
Plasmids		
pRK600	Helper plasmid used for conjugation; ori_{RK2} (*mob*$^+$*tra*$^+$); Cm^r	(38)
pJMT6	mini-Tn*5* delivery plasmid; Amp^r Tel^r	(39)
pSEVA612S	ori_{R6K}; *mob*$^+$; *lacZα*-pUC19/I-SceI; Gm^r	(40)
pSEVA712S	ori_{R6K}; *mob*$^+$; *lacZα*-pUC19/I-SceI; Tmp^r	This work
pSEVAd*prpB*	pSEVA712S carrying a 1.2 kb in-frame deletion fragment of *prpB*	This work
pSEVA228S	ori_{RK2};*mob*$^+$; *xylS; PmI-scel*; Km^r	(40)
pSEVA234	ori_{pBBR1}; *mob*$^+$; *laclq*-P*trc*; Km^r	(40)
pSEVA*icl*	pSEVA234 carrying the *icl1*gene of *M. smegmatis* mc^2 155	This work
pSEVA*prpB*	pSEVA234 carrying the *prpB* gene from *B. ambifaria* T16	This work
pSEVA731	ori_{pBBR1}; *mob*$^+$; Tmp^r	(40)
pSEVA*fuaC*	pSEVA731 carrying the *fuaC* gene from *B. ambifaria* T16	This work
pGPI-SceI	ori_{R6K}; Tmp^r; *mob*$^+$; carries I-SceI cut site	(41)
pGPId*fuaC*	pGPI-SceI carrying a 1.1 kb in frame deletion fragment of *fuaC*	This work
pDAI-SceI	ori_{pBBR1}; Tc^r, *mob*$^+$, carries the gene encoding I-SceI	(41)
Oligonucleotides (5′-> 3′)		
ARB2	GGCCACGCGTCGACTAGTAC	(42)
ARB6	GGCCACGCGTCGACTAGTACNNNNNNNNNNCGCC	(42)
TelBint	GTTGGGCTGGCAGTGTCGATCCGCAA	(32)
TelBext	TTGCGAAGCAGTACCAGCAGGAAT	(32)
KilAint	CCCATGTTCACGCTTTGTTCTTCCAT	(32)
KilAext	CAGATTCGACAGCTCGTTGAGGGA	(32)
prpB3Bamfor	ACGTGGATCCGTGCGAGAAGTGATACCAGTACA	This work
prpB3rev	GGCTATCACGAATACGAGC	This work
prpB5for2	GCTCGTATTCGTGATAGCCCGACAGGTAGACGGCCTTGA	This work
prpB5Nherev	CTAGCTAGCCCTGCATCACGTCGAAGCC	This work
SEVA_marker_rv_U	ATTTAAAUACGTAAATCGTAATTATT	This work

(*Continued on next page*)

TABLE 1 Bacterial strains, plasmids, and oligonucleotides (*Continued*)

Strain, plasmid, or oligonucleotide	Relevant genotype or description	Reference or source
SEVA_marker_fw_U	ACCGTTGUCCTTTTCCGCGCATAACT	This work
TmpR_rv_U	ACAACGGUCCAATTAATTATTAACCCTT	This work
TmpR_fw_U	ATTTAAAUTTGTGTCTCAAAATCTCT	This work
PS3	GAACGCTCGGTTGCCGC	(40)
PS4	AATGACCCCGAAGCAGGG	(40)
P224	GGACAAATCCGCCGCCCT	(40)
P225	AGGGCGGCGGATTTGTCC	(40)
P226	GCGGCAACCGAGCGTTC	(40)
P274	CCTGCTCTGCGAGGCTGG	(40)
P291	CCCTGCTTCGGGGTCATT	(40)
P292	CCAGCCTCGCAGAGCAGG	(40)
prpBcheckfor	TGCAGCAGGTGCAGGAAGTG	This work
prpBNco2	CATGCCATGGATGAGCAACACGCATCTT	This work
prpBdelcheckrv3	CGACGCGTGCGAATACAGGAAC	This work
prpBrevXbaI2	TTACTTCTTGCCCTGCGCGAAC	This work
luc2EcoRIfw5	GGAATTCGCAGACATCGCCGAAACCTC	This work
luc2rv5	CGAGTAGCTATGCCCGACCT	This work
luc2fw3	AGGTCGGGCATAGCTACTCGCGCAACAATATCGTCCGCCC	This work
luc2BamHIrv3	CGGGATCCACACCGGCATTGACGTGCGT	This work
luccheckfw1	AAGCGGGATGCTCGAAGCA	This work
luccheckrv1	CAGCAGCTTGTCGCTTTCGA	This work
iclfwXbaI	GCTCTAGAAGGAGGAAAAACATATGGCAACAATCGAAGCCAAC	This work
iclrvHindIII	CCCAAGCTTTTTCAGTCCTCCTTGCGGAT	This work
prpBfwXbaI	GCTCTAGAAGGAGGCCGTTCATGAGCAACA	This work
prpBrvHindIII	CCCAAGCTTAAAGCGTTCCGGGAACCGT	This work
fuaCfwEcoRI	GGAATTCCGGCAAGGTCGCGGCATGAA	This work
fuaCrvBamHI	CGGGATCCACACCGGAGGACCGCTGTTCGA	This work

medium. These concentrated cell suspensions were used to inoculate Erlenmeyer flasks containing M9 with the addition of different carbon sources (CA, PA, or FA) at an initial OD at 600 nm (OD_{600}) of 0.05 for M9 + CA and M9 + FA, or 0.1 for M9 + PA. Antibiotics and 1 mM IPTG were added to the medium where necessary.

To analyze the growth with FA as the sole nitrogen source, a modified M9 medium without NH_4Cl, and supplemented with 450 µg/mL FA, 0.2% (wt/vol) citrate, 1 mM $MgSO_4$, and 0.1% (vol/vol) metal trace solution, was used.

The MIC of FA was determined after 24 h incubation in M9 + CA, supplemented with antibiotics and IPTG where necessary. All cultures were inoculated at an initial OD_{600} = 0.05 from inocula prepared as described above. The MIC was determined as the minimum concentration of FA that completely inhibited growth. Growth curves and MIC determinations were performed at least in biological triplicates.

Construction of a mini-Tn*5* mutant library; screening and mapping of mini-transposon insertions

To construct a mini-Tn*5* insertional library in *B. ambifaria* T16, plasmid pJMT6 was introduced into *B. ambifaria* by triparental mating as described by Martínez-García et al. (43), with the modifications detailed in Simonetti et al. (44). The selection of transconjugants was performed in LB agar plates containing 20 µg/mL of the antibiotics Tel and Tc. A total of 8,000 transconjugants were screened for the inability to grow with FA as the sole carbon source. Each colony was simultaneously streaked in M9 + CA and M9 + FA agar plates, supplemented with the antibiotics Tel and Tc. After incubation at 32°C for

48 h, colonies unable to grow in M9 + FA were selected. Mapping of mini-Tn*5* insertions was performed by arbitrary primed PCR (42) as previously described (44).

DNA extraction

Genomic DNA from *B. ambifaria* T16 was extracted using the DNeasy Blood & Tissue Kit (Qiagen, Hilton, Germany), according to the protocol provided by the manufacturer. To extract genomic DNA of *Mycobacterium smegmatis* mc^2 155, cells from a fresh plate were resuspended in a buffer containing 100 mM NaCl, 10 mM Tris·HCl pH = 8.0, 1 mM EDTA, and 1% (vol/vol) Triton X-100. For cell lysis, the suspension was incubated at 95°C for 20 min and subjected to three thawing-freezing cycles (5 min at −70°C, followed by 5 min at 100°C). After centrifugation at 13,000 rpm for 5 min, the supernatant was transferred to a new tube, and the DNA was precipitated according to Ausubel et al. (45).

Construction of plasmids and markerless *B. ambifaria* deletion mutants

Primers and vectors used in this work are listed in Table 1. Restriction enzymes were purchased from New England Biolabs Inc. (Ipswich, USA) or Takara Bio Inc. (Shiga, Japan). To construct markerless gene deletions in the genome of *B. ambifaria* T16 two different systems based on the I-SceI endonuclease were used. The deletion of the *prpB* gene was performed by using a suicide vector belonging to the pSEVA (Standard European Vector Architecture) database harboring the Tmp selection marker (46). To construct this plasmid, named pSEVA712S, a DNA fragment carrying the dihydrofolate reductase gene (*dhfrI*) from *E. coli* (GenBank accession number X00926.1) conferring Tmp resistance, was cloned into the pSEVA backbone using the uracil excision methodology (47) as follows. The pSEVA backbone and the *dhfrI* gene, were amplified from pSEVA612S and from a gBlock Gene Fragment carrying *dhfrI* (IDT, Cambridge, USA), respectively, using Phusion U Hot Start DNA polymerase (Thermo Scientific, Waltham, USA) and the primers pairs SEVA_marker_rv_U/SEVA_marker_fw_U or TmpR_rv_U/TmpR_fw_U. Fragments were purified with the NucleoSpin Gel and PCR Clean-up kit (Macherey-Nagel GmbH & Co, Düren, Germany). DNA concentrations were measured using NanoDrop 2000 (Thermo Scientific, Massachusetts, USA). The USER reaction was performed as described by Cavaleiro et al. (47), and incubated at 30°C for 30 min, followed by a touchdown step of 27 cycles at 37°C (−1°C/cycle) for 2 min. The total reaction was used to transform *E. coli* DH5α chemically competent cells. Transformants were selected in LB agar plates containing Tmp and screened for the presence of the Tmp^r marker by colony PCR using primer pairs PS3 and PS4, One Taq DNA polymerase (New England Biolab Inc.), and the protocol provided by the manufacturer. Finally, the pSEVA plasmid carrying the Tmp^r marker was extracted with the NucleoSpin Plasmid Easy Pure (Macherey-Nagel GmbH & Co) and its complete sequence was checked with primers P224, P225, P226, PS3, PS4, P274, P291, and P292 in Eurofins Genomics LLC (Ebersberg, Germany). The new vector, pSEVA712S, was added to the SEVA database (46).

To delete the *prpB* gene of *B. ambifaria* T16, two DNA fragments ≈600 bp flanking the *prpB* gene were amplified with the enzyme Phusion High-Fidelity DNA polymerase (New England Biolabs Inc.), using the primers pairsprpB5Nherev/prpB5for2 and prpB3Bamfor/prpB3rev. The amplified fragments were purified with the Accuprep purification kit (Bioneer Corporation, Korea) and 50 ng of each fragment was used in an overlap-PCR (48) to obtain the 1.2 kb fragment for in-frame deletion. After purification, the fused fragment was cloned in pSEVA712S with the restriction enzymes NheI and BamHI to obtain plasmid pSEVAd*prpB*. This plasmid was introduced into *B. ambifaria* T16 by triparental mating as described by Simonetti et al. (44), with minor modifications. Liquid cultures were grown overnight in 2 mL of LB broth supplemented with the corresponding antibiotics. Cells were washed with 10 mM $MgSO_4$ and mixed in a 1:1:1 ratio into 5 mL of $MgSO_4$ to obtain a final OD_{600} = 0.05 of each strain. Using a syringe, the mixture was concentrated onto a Millipore filter disk, which was placed onto the surface of an LB agar plate. After 16 h of incubation at 30°C, the filter was transferred into 1 mL of 10 mM $MgSO_4$ and suspended by vortexing. The resulting suspension was serially diluted and

plated onto LB agar plates containing Tmp and Tc. Plates were incubated for 48 h at 30°C. The obtained transconjugants colonies were transferred to a fresh plate containing antibiotics and the co-integration of pSEVAd*prpB* into the genome of *B. ambifaria* T16 was evaluated by colony PCR using the primers pairs prpBcheckfor/prpBNco2 and prpBdelcheckrv3/prpBrevXbaI2. Co-integrate resolution was achieved by the introduction of the plasmid pSEVA228S, using the protocol described by Martínez-García and de Lorenzo (49). The deletion of the *prpB* gene was checked by colony PCR using primers prpBcheckfor and prpBdelcheckrv3. One of these mutants was selected and named *B. ambifaria* T42 (Δ*prpB*). Finally, plasmid pSEVA228S was curated from *B. ambifaria* by performing three serial transfers in LB broth without antibiotics, plating serial dilutions in LB agar plates and selecting Km^S colonies.

To delete the *fuaC* gene, DNA regions located upstream and downstream of the gene were amplified with the primers pairs luc2Ecofw5/luc2rv5 and luc2fw3/luc2BamHIrv3, respectively. Both fragments were fused using primers luc2Ecofw5 and luc2BamHIrv3. After digestion with EcoRI and BamHI, the obtained 1,127 bp fragment for in-frame deletion was ligated into pSEVA712S. It was not possible to obtain co-integrate clones using this construct, and plasmid pGPI-SceI was used for generating the *fuaC* deletion instead. Therefore, the 1,127 bp fragment was sub-cloned into pGPI-SceI using EcoRI and XbaI, and the resulting plasmid, pGPId*fuaC*, was introduced into *B. ambifaria* T16 by triparental mating. The integration of pGPId*fuaC* into the genome of *B. ambifaria* T16 was checked with primers pairs luccheckfw1/luc2BamHIrv3 and luc2Ecofw5/luccheckrv1. The co-integrate was resolved by the introduction of plasmid pDAI-SceI. Transconjugants were screened for the loss of Tmp resistance, and Tmp^S clones were subjected to colony-PCR with primers luccheckfw1 and luccheckrv1 in order to verify the deletion of the *fuaC* gene in the genome of *B. ambifaria*. One of these double-crossover mutants was selected and named *B. ambifaria* T800. Finally, curation of pDAI-SceI was performed as described by Flannagan et al. (41).

To construct plasmid pSEVA*icl* bearing the *icl1* gene (encoding the enzyme *iso*citrate lyase from *M. smegmatis* mc^2 155) under the *laclq*-P*trc* inducible promoter, the gene was amplified using primers iclfwXba and iclrvHindIII, digested and ligated into the expression plasmid pSEVA234. To obtain the plasmid pSEVA*prpB*, the *prpB* gene of *B. ambifaria* T16 was amplified with primers prpBfwXbaI and prpBrvHindIII, digested and ligated into pSEVA234. Finally, complementation of the *fuaC* deletion was performed with plasmid pSEVA*fuaC*. In this case, a 1,475 bp fragment, which includes the *fuaC* coding sequence of *B. ambifaria* T16 and its promoter region, was amplified with the primer pair fuaCfwEcoRI/fuaCrvBamHI, digested and ligated into pSEVA731.

FA toxicity assay using barley seedlings

Barley seeds were surface-disinfected with 0.2% (vol/vol) NaClO, submerged in sterile deionized water for 1.5 h and placed inside a humid chamber for 24 h to allow germination. The effect of FA on the growth of barley seedlings was evaluated as described by Simonetti et al. (32) using M9, M9 + FA, and cell-free supernatants from stationary phase cultures of *B. ambifaria* strains cultivated in M9 + FA.

Identification of differentially induced proteins during growth with FA as the sole carbon source

Three independent cultures of *B. ambifaria* T16 were cultivated in M9 + CA and M9 + FA to an $OD_{600} \approx 0.7$. Cells were harvested at 4°C, washed with ice-cold 10 mM Tris·HCl pH = 7.5, resuspended in Lysis Buffer (10 mM Tris·HCl pH = 7.5, 1 mM PMSF, 100 µg/mL lysozyme, 1 mM DMSO, and 1 mM EDTA), and mechanically disrupted using glass beads. The obtained protein extracts were lyophilized, and subjected to trypsin digestion and clean-up using the iST 8 × kit (PreOmics GmbH, Martinsried, Germany), and the protocol provided by the manufacturer. Protein samples were analyzed by LC-MS as described elsewhere (50).

MaxQuant 2.1.2.0 was used to identify and quantify the proteins by LFQ with the following parameters: Database NCBI_Burkholderia_ambifaria_RQYA01.1_20220630; MS tol, 10 ppm; MS/MS tol, 20 ppm Da; Peptide FDR, 0.1; Protein FDR, 0.01 Min. peptide Length, 7; Variable modifications, Oxidation (M); Fixed modifications, Carbamidomethyl (C); Peptides for protein quantitation, razor and unique; Min. peptides, 1; Min. ratio count, 2. The quantitative protein abundance data (MaxQuant LFQ values) were analyzed by performing an adjusted two-sample *t* test as described in Perseus (51). *P* values lower than 0.05 were considered significant. Finally, the proteomic data were uploaded in the pathway genome database (PGDB) of *B. ambifaria* T16 previously constructed (52), by using the Omics module of the Pathway Tool software v. 25 (53).

RESULTS

Transposon mutagenesis and mapping of mini-Tn*5* insertion sites in mutants unable to grow with FA as the sole carbon and energy source

With the aim to find genes involved in FA catabolism and FA tolerance in *B. ambifaria* T16, two different experimental approaches were used. First, we constructed a mini-Tn*5* insertional library to select mutants unable to grow in M9 + FA. After plating and incubation, eight clones from the insertional library were unable to grow on FA as carbon source. The coordinates of the mini-Tn*5* insertions and the genes interrupted by the transposon in these mutants are shown in Table 2. In four of these insertional mutants (*B. ambifaria* FA2, *B. ambifaria* FA4, *B. ambifaria* FA91, and *B. ambifaria* FA92), the transposon insertion mapped in different genes encoding components of the 2-methylcitrate cycle (2-MCC; Table 2 and Fig. 1A). The 2-MCC is an anaplerotic pathway widely distributed among bacteria and fungi, where propionyl-coenzyme A (CoA) is converted to pyruvate and succinate. In *B. ambifaria* T16, the *prp* locus comprises the *prpR* gene, encoding the σ^{54}-dependent transcriptional activator of the *prp* genes (54), and four structural genes, *prpB*, *prpC*, *acnD,* and *prpF*, encoding the enzymes involved in propionyl-CoA metabolism (Fig. 1A and B).

In *B. ambifaria* FA3, the mini-Tn*5* cassette interrupted the gene EIB72_01775, encoding the outer membrane lipid asymmetry maintenance protein MlaD. MlaD is part of the highly conserved Mla (maintenance of lipid asymmetry) system (56), involved in the maintenance of outer membrane lipid asymmetry in Gram-negative bacteria.

TABLE 2 Location of mini-Tn*5* Tel insertions in *B. ambifaria* mutants unable to grow with FA as the sole carbon and energy source

Mutant	Interrupted gene (GenBank Locus Tag) (strand)[a]	Gene	Putative function[b]	Coordinates of insertion (scaffold)[c]
B. ambifaria FA2	EIB72_27350 (–)	*prpB*	2-methyl*iso*citrate lyase	236678 (scaffold 9)
B. ambifaria FA3	EIB72_01775 (+)	*mlaD*	Outer membrane lipid asymmetry maintenance protein	88315 (scaffold 2)
B. ambifaria FA4	EIB72_27355 (+)	*prpR*	Propionate catabolism operon regulatory protein	238068 (scaffold 9)
B. ambifaria FA21	EIB72_16280 (+)		Acyl-CoA dehydrogenase	115004 (scaffold 6)
B. ambifaria FA84	EIB72_11905 (+)		Phosphoenolpyruvate carboxylase	214877 (scaffold 4)
B. ambifaria FA90	Intergenic region EIB72_05180–85		-	592108 (scaffold 3)
B. ambifaria FA91	EIB72_27335 (–)	*prpF*	2-methylaconitate isomerase	232072 (scaffold 9)
B. ambifaria FA92	EIB72_27355 (+)	*prpR*	Propionate catabolism operon regulatory protein	238495 (scaffold 9)

[a]The sign + or – refers to the DNA strand encoding the gene.
[b]Predicted functions are based on the annotation of *B. ambifaria* T16 genome using the RAST server (55).
[c]Genomes coordinates in *B. ambifaria* T16 genome (GenBank accession number RQYA00000000).

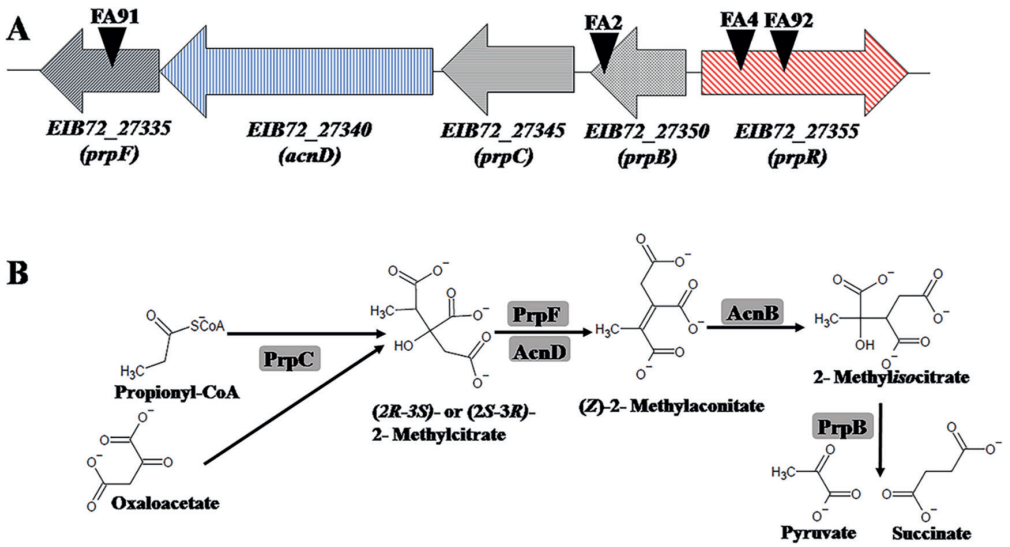

FIG 1 (A) Genomic organization of the *prp* locus in *B. ambifaria* T16 and localization of mini-Tn*5* insertions in the mutants *B. ambifaria* FA2, FA4, FA92, and FA91. Genes are represented by arrows and black inverted triangles represent the localization of the mini-Tn*5* insertions in each mutant. (B) 2-Methylcitrate cycle in *B. ambifaria* T16. Enzymes are shaded in gray rectangles. PrpC: methylcitrate synthase, AcnD: methylcitrate dehydratase, PrpF: methylaconitate *cis-trans* isomerase, AcnB: aconitase, PrpB: methyl*iso*citrate lyase. The AcnB enzyme is not encoded in the *prp* locus.

In *B. ambifaria* FA21, the mini-Tn*5* mapped in locus EIB72_16280. This gene is predicted to encode an acyl-CoA dehydrogenase. In *B. ambifaria* FA84, the transposon interrupted gene EIB72_11905, which encodes the enzyme phosphoenolpyruvate carboxylase (PEPC). In close proximity to EIB72_11905, genes predicted to be involved in the transport and catabolism of aromatic compounds were found. Finally, the mutant *B. ambifaria* FA90 bears a mini-Tn*5* insertion in an intergenic region between two genes encoding enzymes involved in RNA processing, degradation, and modification (RNase E/G family endoribonuclease and RluA family pseudouridine synthase) (57, 58).

Tolerance to FA and ability to grow on FA as the sole nitrogen source in *B. ambifaria* insertional mutants

As mentioned above, FA is toxic to different types of cells and negatively affects diverse cellular functions. Therefore, the growth impairment observed with FA as the sole carbon and energy source in the insertional mutants could be attributed to the inactivation of a gene involved in FA catabolism or a gene required to tolerate the exposure to this mycotoxin. For that reason, the MIC of FA was determined in cultures of the wild-type strain (*B. ambifaria* T16) and the insertional mutants. Table 3 shows that two insertional mutants, *B. ambifaria* FA2 (*prpB*::mini-Tn*5*Tel) and *B. ambifaria* FA3 (*mlaD*::mini-Tn*5*Tel), were more sensitive to the presence of FA in the growth medium than the wild-type strain. While *B. ambifaria* T16 showed a MIC of 1,600 µg/mL, the MIC obtained for *B. ambifaria* FA2 and FA3 was 200 µg/mL In the remaining insertional mutants, the tolerance to FA was similar to that obtained for the wild-type strain (Table 3). Next, we decided to analyze the growth of the insertional mutants with FA as the sole nitrogen source. With this purpose in mind, the strains were cultivated in a modified M9 minimal medium without the addition of NH_4Cl, supplemented with 0.2% (wt/vol) citrate (carbon source) and 450 µg/mL FA (carbon source and sole nitrogen source) (32). Only *B. ambifaria* FA84, which possesses a mini-Tn*5* insertion in a gene predicted to encode PEPC, was able to reach an OD_{600} similar to the wild-type strain (Table 3). As expected, *B. ambifaria* FA2 and FA3 were unable to grow with 450 µg/mL FA as sole nitrogen source. This result is in agreement with the FA MIC values obtained for these mutants (Table 3). Another strain unable to grow with FA as nitrogen source was *B. ambifaria* FA21.

TABLE 3 MICs of FA and capability to grow with FA as carbon and nitrogen source for *B. ambifaria* T16 (wt) and mini-Tn*5* insertional mutants

B. ambifaria strain	MIC FA (µg/mL)	Growth with FA as carbon source	Growth with FA as nitrogen source Final OD_{600}[a]
T16 (wild type)	1,600	+	1.26 ± 0.27
FA2 (*prpB*::mini-Tn*5*Tel)	200	-	0.11 ± 0.05
FA3 (*mlaD*::mini-Tn*5*Tel)	200	-	0.05 ± 0.01
FA4 (*prpR*::mini-Tn*5*Tel)	1,600	-	0.65 ± 0.06
FA21 (EIB72_16280::mini-Tn*5*Tel)	1,600	-	0.07 ± 0.01
FA84 (EIB72_11905::mini-Tn*5*Tel)	1,600	-	1.22 ± 0.22
FA90 (EIB72_05180–85::mini-Tn*5*Tel)	1,600	-	0.81 ± 0.04
FA91 (*prpF*::mini-Tn*5*Tel)	1,600	-	0.81 ± 0.04
FA92 (*prpR*::mini-Tn*5*Tel)	1,600	-	0.62 ± 0.07

[a]Mean ± SD of three independent cultures is shown.

This strain possesses a mini-Tn*5* insertion in EIB72_16280, which encodes a predicted acyl-CoA dehydrogenase. The cell densities of the remaining mutants were lower than those of the wild-type, indicating that the transposon insertions, not only completely prevent growth with FA as sole carbon source, but also negatively affect the capability to grow with FA as the sole nitrogen source.

Construction of a *B. ambifaria prpB* deletion mutant and evaluation of its ability to grow on FA

The results obtained with the insertional mutants pointed to an important role of the 2-MCC in the capability to grow with FA as the sole carbon source. To provide genetic evidence supporting this phenotype, the gene *prpB*, encoding methyl*iso*citrate lyase (the last enzyme of the 2-MCC; Fig. 1), was deleted. The *B. ambifaria* Δ*prpB* strain obtained was named *B. ambifaria* T42. In agreement with the results obtained with all the mutants with insertions in the *prp* locus, *B. ambifaria* T42 was also unable to grow in M9 + FA. Furthermore, the *prpB* deletion also negatively affected the tolerance to FA (Table 4), as the MIC obtained for this strain was 400 µg/mL, much lower than the value obtained for the wild-type strain (1,600 µg/mL) (Table 3).

Then, we decided to perform two different complementation tests, one by introducing the *prpB* gene of *B. ambifaria* T16, and the other by introducing a gene from a different bacterial species encoding an enzyme with methyl*iso*citrate lyase activity into the Δ*prpB* mutant. This functional complementation was performed with the *icl1* gene of *M. smegmatis* mc^2 155. This gene was chosen because it encodes an enzyme with reported *iso*citrate lyase and methyl*iso*citrate lyase activities (59). The *prpB* and *icl1* genes were separately cloned in an inducible expression plasmid and introduced into *B. ambifaria* T42. Table 4 indicates that the introduction of plasmids pSEVA*icl* and

TABLE 4 MICs of FA, capability to grow with FA as carbon source and specific growth rates (µ) calculated for *B. ambifaria* strains

B. ambifaria strain/plasmid	MIC FA (µg/mL)	$\mu_{CA\ C.\ source}$[a] (h^{-1})	$\mu_{PA\ C.\ source}$[b] (h^{-1})	$\mu_{FA\ C.\ source}$[c] (h^{-1})	$\mu_{FA\ N.\ source}$[d] (h^{-1})
T42 (Δ*prpB*)	400	ND[e]	ND	ND	ND
T16/pSEVA234	1,600	0.40 ± 0.020	0.04 ± 0.004	0.19 ± 0.013	ND
T42/pSEVA234	400	0.42 ± 0.022	0	0	ND
T42/pSEVA*icl*	1,600	0.37 ± 0.020	0.03 ± 0.004	0.09 ± 0.010	ND
T42/pSEVA*prpB*	3,200	0.42 ± 0.024	0.19 ± 0.011	0.14 ± 0.047	ND
T16/pSEVA731	1,600	ND	ND	0.20 ± 0.018	0.17 ± 0.006
T800/pSEVA731	1,600	ND	ND	0	0
T800/pSEVA*fuaC*	1,600	ND	ND	0.24 ± 0.046	0.13 ± 0.005

[a]µ Sodium citrate as carbon source.
[b]µ Sodium propionate as carbon source.
[c]µ Fusaric acid as carbon source.
[d]µ Fusaric acid as nitrogen source.
[e]ND: not determined.

pSEVA*prpB* in the Δ*prpB* mutant increased the tolerance to FA. The MIC value obtained for *B. ambifaria* T42/pSEVA*icl* (1,600 µg/mL) was similar to that of the wild-type strain. Interestingly, *B. ambifaria* T42/pSEVA*prpB* showed a higher MIC value than the wild type (3,200 µg/mL).

Next, we compared the growth of *B. ambifaria* T16/pSEVA234, *B. ambifaria* T42/pSEVA234, *B. ambifaria* T42/pSEVA*icl*, and *B. ambifaria* T42/pSEVA*prpB* in minimal medium with CA, PA, or FA as carbon and energy sources (Fig. 2 and Table 4). As shown in Fig. 2A and Table 4, the wild-type strain, the Δ*prpB* mutant carrying the vector plasmid and the mutant bearing pSEVA*prpB* showed very similar growth profiles and almost identical specific growth rates when they were cultivated with CA as the sole carbon source. Meanwhile, the growth rate of the Δ*prpB* strain carrying pSEVA*icl* was slightly lower than the obtained for the other strains. Different results were obtained when these strains were grown with PA as the sole carbon source (Fig. 2B and Table 4). Severe growth impairment was observed for *B. ambifaria* T42/pSEVA234. The introduction of *prpB* or the *icl1* gene in the T42 strain restored growth in PA. Besides, as it was observed with CA, the growth rate of strain T42/pSEVA*icl* was lower than the growth rates obtained for strains T16/pSEVA234 and T42/pSEVA*prpB*. Moreover, *B. ambifaria* T42 carrying pSEVA*prpB* showed a much higher growth rate and a shortened lag phase compared to the wild type strain. Finally, similar results to the ones obtained with PA were observed when FA was used as the sole carbon and energy source (Fig. 2C and

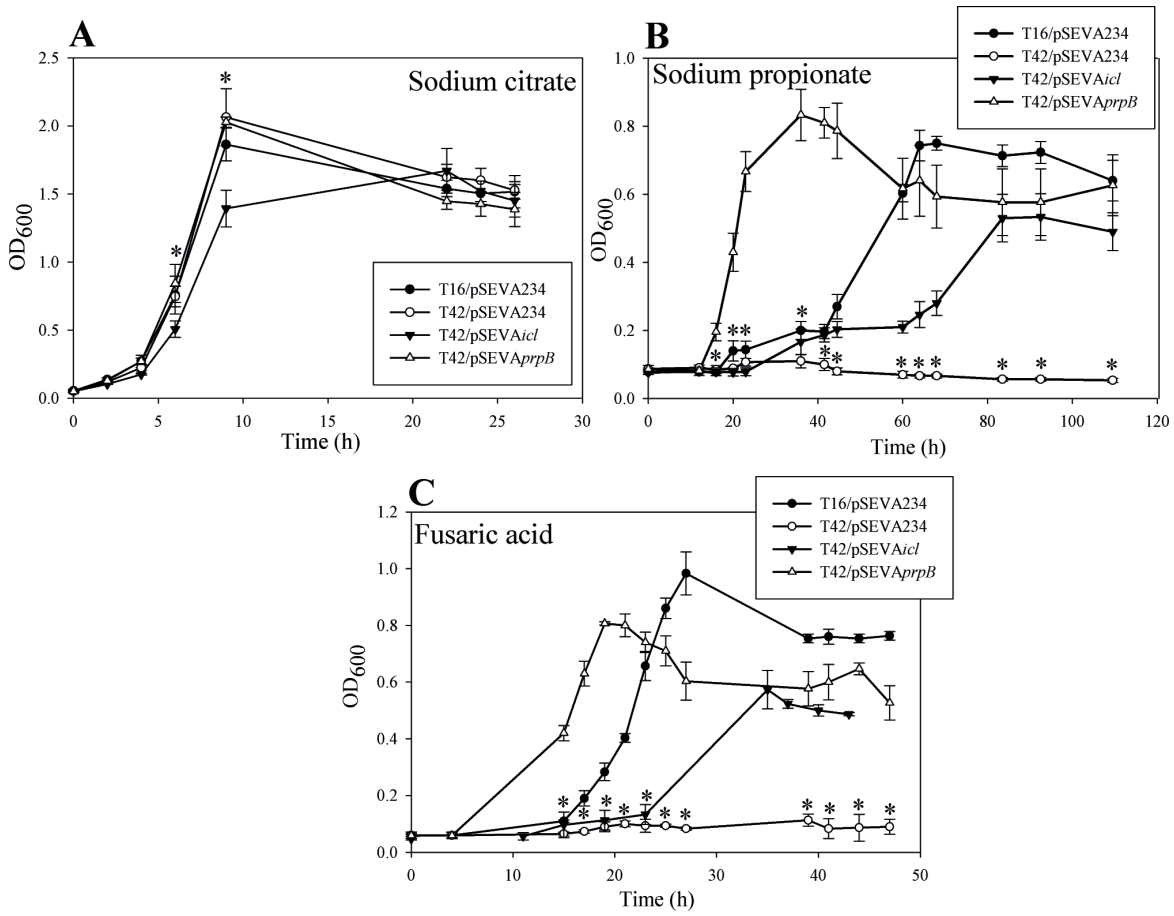

FIG 2 Growth of *B. ambifaria* strains in M9 minimal medium with 0.2% (wt/vol) sodium citrate (**A**), 0.2% (wt/vol) sodium propionate (B) or 450 µg/mL fusaric acid (C) as sole carbon and energy source. The graphs show the means ± SD obtained from three biological replicates. The OD_{600} values obtained were subjected to Kruskal-Wallis analysis of variance followed by Dunnett's test. The Δ*prpB* strain bearing the vector plasmid (T42/pSEVA234) was used as control in the test. *P* values were considered significant when they were lower than 0.05. Asterisks indicate that there is a statistically significant difference between OD_{600} values of strains T16/pSEVA234, T42/pSEVA*icl* or T42/pSEVA*prpB* and OD_{600} values of T42/pSEVA234.

Table 4). The *prpB* deletion mutant carrying pSEVA234 was unable to grow using FA as carbon source. The introduction of pSEVA*icl* or pSEVA*prpB* in the Δ*prpB* strain was able to restore the growth with FA. Over-expression of *prpB* shortened the lag phase. These results indicate that a functional 2-MCC is essential for the growth of *B. ambifaria* T16 with FA as the sole carbon and energy source, and suggest that propionyl-CoA is generated during FA catabolism.

Proteins differentially induced during growth with FA as the sole carbon source

A proteomic analysis of *B. ambifaria* T16 grown with CA or FA as the sole carbon and energy source was performed to identify proteins involved in FA catabolism. A detailed list of the identified proteins (1,998 proteins), and the difference in protein abundance between the two cultivation conditions are shown in Table S1 in the supplemental material. Several enzymes involved in fatty acid biosynthesis and cofactor biosynthesis (including coenzyme A and flavin biosynthesis) were upregulated during growth of *B. ambifaria* T16 with FA. Furthermore, a higher abundance of enzymes involved in degradation of amino acids, carboxylates, and lipids was observed when the bacteria used the mycotoxin as the sole carbon and energy source (Fig. S1; supplemental material).

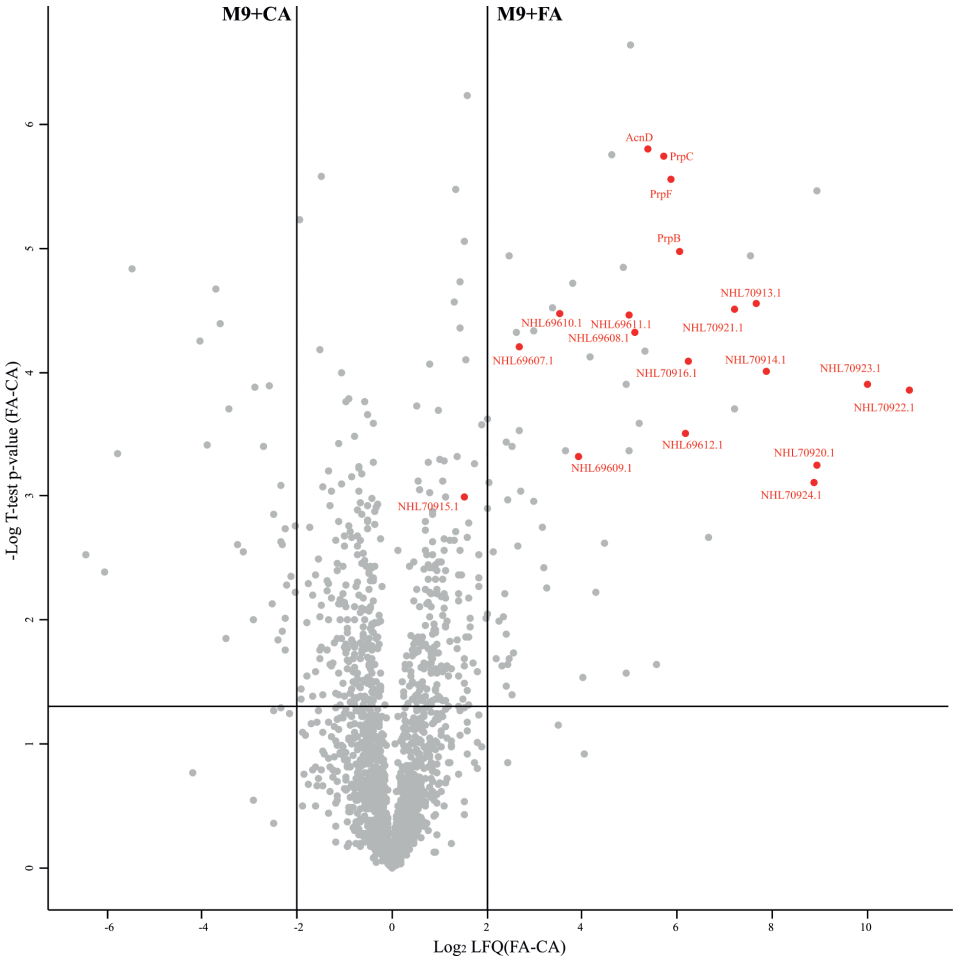

FIG 3 Differential protein abundance in *B. ambifaria* T16 grown in M9 minimal medium with citrate (M9 + CA) or fusaric acid (M9 + FA) as sole carbon source. Red dots represent some upregulated proteins during growth with FA. Proteins IDs NHL69607.1 to NHL69612.1 correspond to proteins involved in valine degradation. Proteins NHL70913.1 to 70915.1: 2-oxo acid dehydrogenase complex. NHL70916.1: predicted BdkR transcriptional regulator involved in the regulation of isoleucine and valine catabolism. Proteins NHL70920.1 to 70924.1 are encoded in a gene cluster of unknown function.

Fig. 3 shows the proteomic results as a volcano plot. Enzymes belonging to the 2-MCC showed a log_2LFQ(FA-CA)=5–6, indicating a much higher intracellular level of these proteins during growth with FA compared to CA. Some proteins encoded in a gene cluster predicted to be involved in valine degradation (NHL69607.1 to NHL69612.1) were also found to be significantly upregulated during growth with FA (Fig. 3 ; Table S1). Other proteins that showed very high levels of abundance during the growth of *B. ambifaria* T16 with FA, with log_2LFQ(FA-CA) values from 6.2 to 10.8, include NHL70913.1, NHL70914.1, NHL70916.1, and NHL70920.1 to NHL70924.1 (Fig. 3 ; Table S1). Protein NHL70916.1 is predicted to be a BdkR transcriptional factor involved in the regulation of isoleucine and valine catabolism, and proteins NHL70913.1 and NHL70914.1 belong to a 2-oxoacid dehydrogenase complex. These complexes convert 2-oxoacids to the corresponding acyl-CoA derivatives. Proteins NHL70920.1 to 70924.1, encoded in the gene cluster EIB72_31580 to EIB72_31610, have no known function. The genetic organization and the predicted functions of the proteins encoded in this cluster are shown in Fig. 4 and Table 5. The gene EIB72_31580 encodes a predicted transcriptional regulator of the AraC family. This regulator possesses 38% identity to the NimR regulator of *E. coli* involved in the tolerance to 2-nitroimidazole (60). Downstream of this regulatory gene, six genes encoding enzymes with different activities are found (Fig. 4). Among them, EIB72_31585 and EIB72_31600 are predicted to encode two enoyl-CoA hydratases. These proteins identified as NHL70920.1 and NHL70923.1, possess sequence identities values of 36 and 34%, respectively, to the 2,3-dehydroadipyl-CoA hydratase and 1,2-epoxyphenylacetyl-CoA isomerase of *E. coli*, which are involved in the catabolism of phenylacetate (61). The protein encoded by EIB72_31590 belongs to the creatininase family, which includes proteins catalyzing the hydrolysis of an amide bond (62, 63). The gene EIB72_31595 is predicted to encode a flavin-dependent oxidoreductase (NHL70922.1) from the luciferase-like monooxygenase (LLM) family. According to a classification based on their structural and functional characteristics, members of the LLM belong to group C Flavin-dependent monooxygenases (FMOs-C) (64). These proteins use reduced FMN for the activation of molecular oxygen, which is generated by a NAD(P)H-dependent flavin reductase (64). A gene predicted to encode a flavin-reductase (EIB72_31610) with an FMN binding site is also located in this gene cluster (Fig. 4). The flavin reductase encoded by EIB72_31610 has 45.6% identity to the NADH-FMN reductase RutF of *E.coli*, involved in the catabolism of uracil (65). Finally, the gen EIB72_31605 encodes a predicted AMP binding protein with high sequence identity to long-chain fatty acid-CoA ligases.

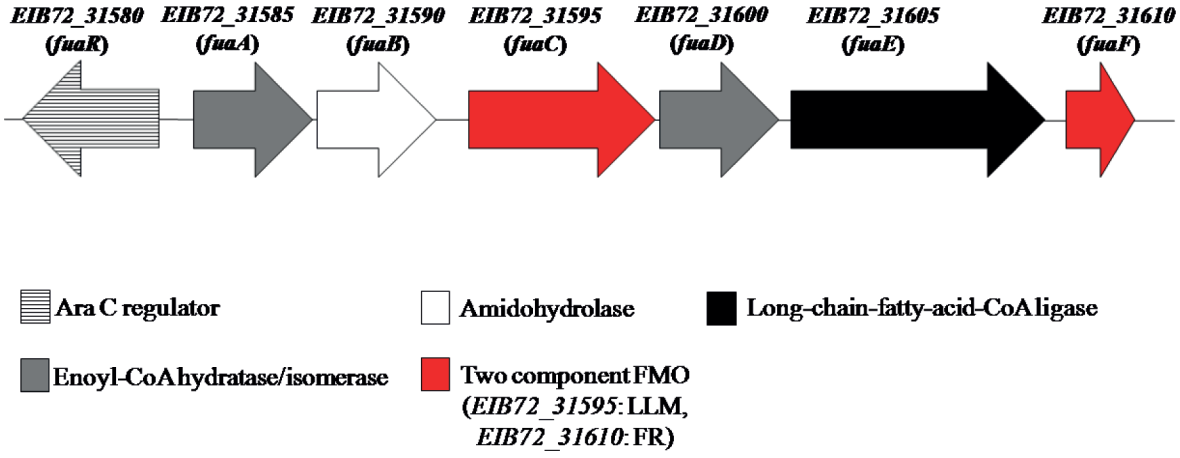

FIG 4 Organization of the gene cluster EIB72_31580-EIB72_31610 (*fua* cluster) encoding proteins NHL70920.1 to 70924. 1. Genes are represented by arrows. Locus IDs are shown above the genes. FR, flavin reductase; LLM, luciferase-like monooxygenase.

TABLE 5 Functional annotations of the proteins encoded by the EIB72_31580 to EIB72_31610 (*fua*) gene cluster

Gene locus	Protein ID	Protein length (aa)	Putative funcion	Conserved domains/interval[a]	Nearest Homolog/ accession Nos[ob]	Identity (%)
EIB72_31580 (*fuaR*)	NHL70919.1	273	AraC family transcriptional regulator	Cupin_NimR (40–121) AraC family (147–272)	HTH-type transcriptional regulator NimR (*E. coli* K-12)/P76241.1	38.49
EIB72_31585 (*fuaA*)	NHL70920.1	254	Enoyl-CoA hydratase/ Isomerase family protein	Crotonase (7–194)	2,3-dihydroadipyl-CoA hydratase (*E. coli* K-12)/P76082.1	36.62
EIB72_31590 (*fuaB*)	NHL70921.1	259	Creatininase family protein (amido-hydrolase)	Creatininase (22–250)	Mycofactocin precursor peptide peptidase (*Mycobacterium ulcerans* Agy99)/A0PM51.1	33.33
EIB72_31595 (*fuaC*)	NHL70922.1	384	LLM class flavin-dependent oxidoreductase	Bac-luciferase (3–324)	Uncharacterized protein y4vj (*Synorhizobium fredii* NGR234)/ Q53218.2	25.22%
EIB72_31600 (*fuaD*)	NHL70923.1	262	Enoyl-CoA hydratase/isomerase family protein	Crotonase (6–254)	Probably enoyl-CoA hydratase (*Caenorhabditis elegans*)/P34559.1	35.25
EIB72_31605 (*fuaE*)	NHL70924.1	635	AMP binding protein	Adenylate forming domain-ClassI superfamily (16–624)	Putative fatty-acid-CoA ligase (*Mycobacterium tuberculosis*)/P9WQ52.1	33.79
EIB72_31610 (*fuaF*)	-	154	Flavin reductase (pseudogen)	Pyridoxine 5′-phosphate oxidase and flavin reductase (1–149)	FMN reductase (NADH) RutF (*Yersina enterocolitica* 8081)/ A1JMW4.1	49.04

[a]The proteins sequences were analyzed against the Conserved Domain Database at the NCBI website. Intervals correspond to aminoacid sequence numbers.
[b]Top BLASTP hit obtained using the UniProtKB/Swiss-Prot Database at the NCBI website.

Construction of a *B. ambifaria* deletion mutant in the gene encoding the LLM NHL70922.1 and evaluation of its capability to grow on FA

According to *in silico* predictions, the genes EIB72_31595 and EIB72_31610 encode a two-component FMO from the LLM family. Two-component FMOs catalyze the oxidation of several substrates, including N-heterocyclic compounds (65–68). The LLM NHL70922.1 possesses 25% identity to the pyrimidine monooxygenase RutA of *E. coli* (65), 34% identity to the tetramethyl pyrazine oxygenase TpdA of *Rhodococcus* sp. THP1 (67), 29% to the pyridine monooxygenase PyrA of *Arthrobacter* sp. 68b (66), and 23% to the trigonelline monooxygenase TgnB of *Acitenobacter baylyi* ADP1 (68). We hypothesized that the products of the gene cluster EIB72_31580-EIB72_31610 are involved in the first steps of FA catabolism in *B. ambifaria* T16. To find out if NHL70922.1 is involved in the catabolism of FA, we constructed a clean deletion mutant in the gene encoding this protein (EIB72_31595). This new strain was designated *B. ambifaria* T800. Next, a DNA fragment encompassing the gene locus EIB72_31595 and its promoter region was cloned in pSEVA731 and introduced into *B. ambifaria* T800. The MICs of FA and the capability to grow with the mycotoxin were analyzed in *B. ambifaria* T16 and T800 carrying pSEVA731 and in *B. ambifaria* T800 with the pSEVA plasmid carrying the EIB72_31595 gene fragment. *B. ambifaria*T800/pSEVA731 showed the same MIC for FA as T16/pSEVA731 (Table 4), indicating that deletion of EIB72_31595 does not affect the tolerance of *B. ambifaria* to this mycotoxin. However, elimination of EIB72_31595 completely abolished the capability of *B. ambifaria* to grow with FA as the sole carbon and energy source (Fig. 5A). Introduction of pSEVA731 carrying EIB72_31595 into *B. ambifaria* T800 was able to restore growth (Fig. 5A), demonstrating that EIB72_31595 is essential for FA catabolism in *B. ambifaria* T16. For that reason, we decided to designate the gene cluster encompassing EIB72_31580-EIB72_31610 as *fua* (*fu*saric *a*cid) cluster and the gene EIB72_31595 as *fuaC*. As it can be observed in Fig. 5A and Table 4, the

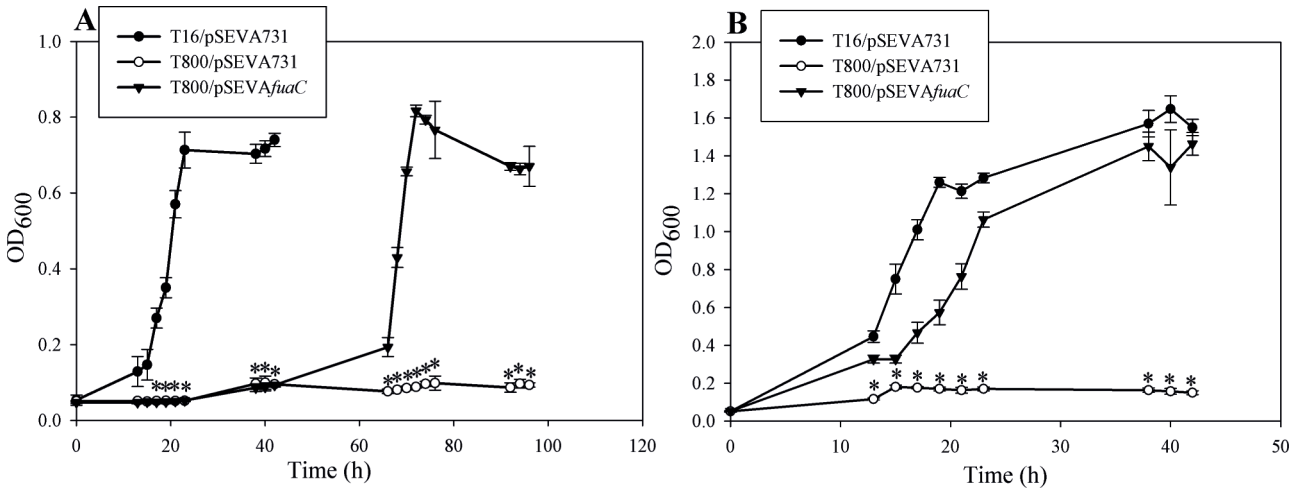

FIG 5 Growth of *B. ambifaria* strains with fusaric acid as the sole carbon and energy source (A) or as the sole nitrogen source (B). The graphs show the means ± SD obtained from three biological replicates. OD_{600} values were subjected to Kruskal-Wallis analysis of variance, followed by Dunnett's test. *B. ambifaria* T800/pSEVA731 was used as a control in the test. *P* values were considered significant when they were lower than 0.05. Asterisks indicate that there is a statistically significant difference with *B. ambifaria* T800/pSEVA731.

wild-type strain with the vector plasmid (*B. ambifaria* T16/pSEVA731) and the complemented strain (*B. ambifaria* T800/pSEVA*fuaC*) grew at very similar specific growth rates. A very long lag phase, which lasted more than 40 h, was observed when *B. ambifaria*T800/pSEVA*fuaC* was cultivated with FA as the sole carbon source (Fig. 5A).

As expected, the deletion of the *fuaC* gene also eliminated the capability of *B. ambifaria* to grow with FA as the sole nitrogen source (Fig. 5B). Growth was restored by the introduction of pSEVA*fuaC*. *B. ambifaria* T800 bearing pSEVA*fuaC* showed a slightly lower growth rate than the wild-type strain carrying the vector plasmid (Table 4).

Due to its reported phytotoxic effects, the presence of FA can be detected by employing simple phytotoxicity assays (8, 10, 11, 13, 32). Taking this into account, we evaluated the presence of FA in the culture supernatants of *B. ambifaria* T16/pSEVA731, *B. ambifaria* T800/pSEVA731, and *B. ambifaria* T800/pSEVA*fuaC* cultivated with FA as the sole carbon and energy source, by applying the cell-free supernatants on germinated barley seedlings (32)(Fig. 6A and B). The growth medium with the addition of 450 µg/mL FA (M9 + FA) was used as a control of the experiment. As expected, the growth of the roots and the coleoptile of barley seedlings was negatively affected by the treatment with M9 + FA (Fig. 6A and B). Barley seedlings treated with cell-free-supernatants from stationary phase-cultures of *B. ambifaria* T800/pSEVA731 showed similar coleoptile's and root's lengths to the seeds treated with M9 + FA, indicating that FA is present in the supernatant and therefore has not been catabolized by this strain. Meanwhile, the barley seedlings exposed to the cell-free-supernatants from stationary phase-cultures of *B. ambifaria* T16/pSEVA731 or *B. ambifaria* T800/pSEVA*fuaC* cultivated with FA, showed coleoptiles and roots significantly longer than the barley seedlings exposed to M9 + FA, showing that FA has been degraded in cultures of these strains.

DISCUSSION

This work describes the first example of bacterial genes essential for growth on FA as the sole carbon and energy source. By screening of a transposon insertional library, several mini-Tn*5* mutants of *B. ambifaria* were found to be unable to grow in minimal medium with 450 µg/mL FA as the sole carbon source. Among these mutants, *B. ambifaria* FA2 and FA3 showed an enhanced sensitivity to FA. Moreover, none of these mutants were able to grow with 450 µg/mL FA as the sole nitrogen source.

In *B. ambifaria* FA3, the mini-Tn*5* insertion mapped in *mlaD*, a gene encoding one of the periplasmic components of the Mla system. This system is composed of

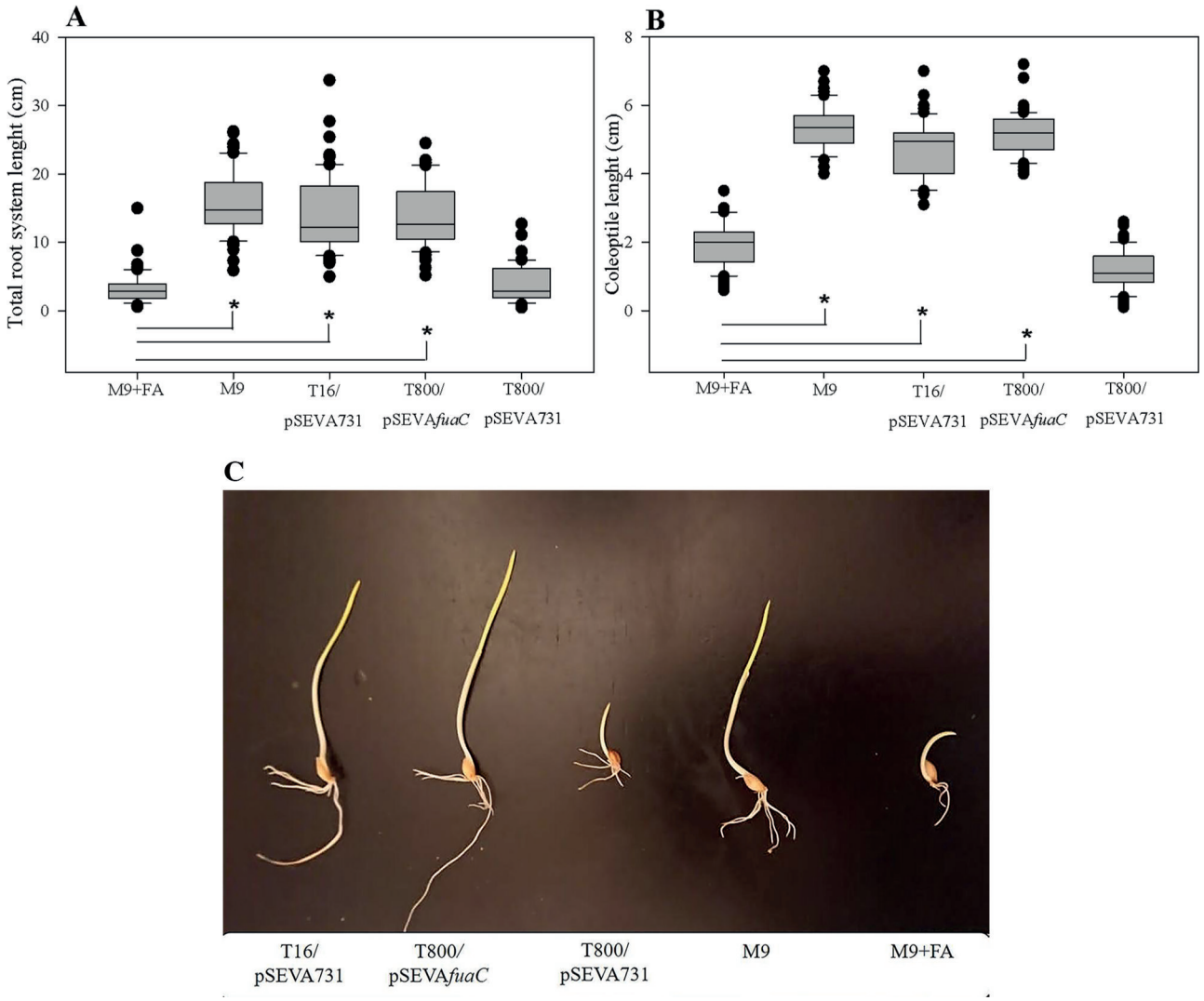

FIG 6 FA toxicity assay using barley seedlings. Box plots of median, 1st and 3rd quartiles (boxes), and 1.5x quartiles (whiskers) corresponding to total root lenght (A) and coleoptile length (B) of seedlings (n=60) treated with cell-free supernatants from stationary phase-cultures of *B. ambifaria* strains, M9 minimal medium (M9), or M9 supplemented with 450 µg/mL FA (M9+FA). Three biological replicates were used. Dots denote observations outside the range of adjacent values. Data were subjected to Kruskal-Wallis analysis of variance and compared by Dunnet's test. Seeds treated with M9 + FA were used as control. Asterisks indicate significant differences at $P < 0.05$ between values from the barley seedlings treated with bacterial supernatants or M9, and the barley seedlings treated with M9 + FA (control). (C) Photographic image showing barley seedlings treated with culture supernatants of *B. ambifaria* strains, M9 minimal medium (M9), or M9 supplemented with 450 µg/mL FA (M9 + FA).

six proteins distributed across the cell envelope and functions as an intermembrane phospholipid transport system that maintains lipid asymmetry in the outer membrane (OM) of Gram-negative bacteria (56). This asymmetry, established by having phospholipids confined to the inner leaflet of the membrane and lipopolysaccharides to the outer leaflet, is crucial to the barrier function of the OM. Mutants defective in the Mla pathway are hypersensitive to detergents (56), hydrophobic compounds (69), antibiotics and human serum (70). Besides enhanced sensitivity to FA, the growth of *B. ambifaria* FA3 was also affected by the presence of toluene and SDS/EDTA (Supplemental material; Table S2 and Table S3). Although the effects of FA on the cell envelope of Gram-negative bacteria have not been evaluated so far, the structure of this mycotoxin, its ability to bind metal cations with high affinity (23), and its oxidative power (11), point to a probable OM disruptive effect. In this scenario, the Mla system would be very important to preserve the integrity of the OM (Fig. 7) . The importance of the OM in the tolerance to FA

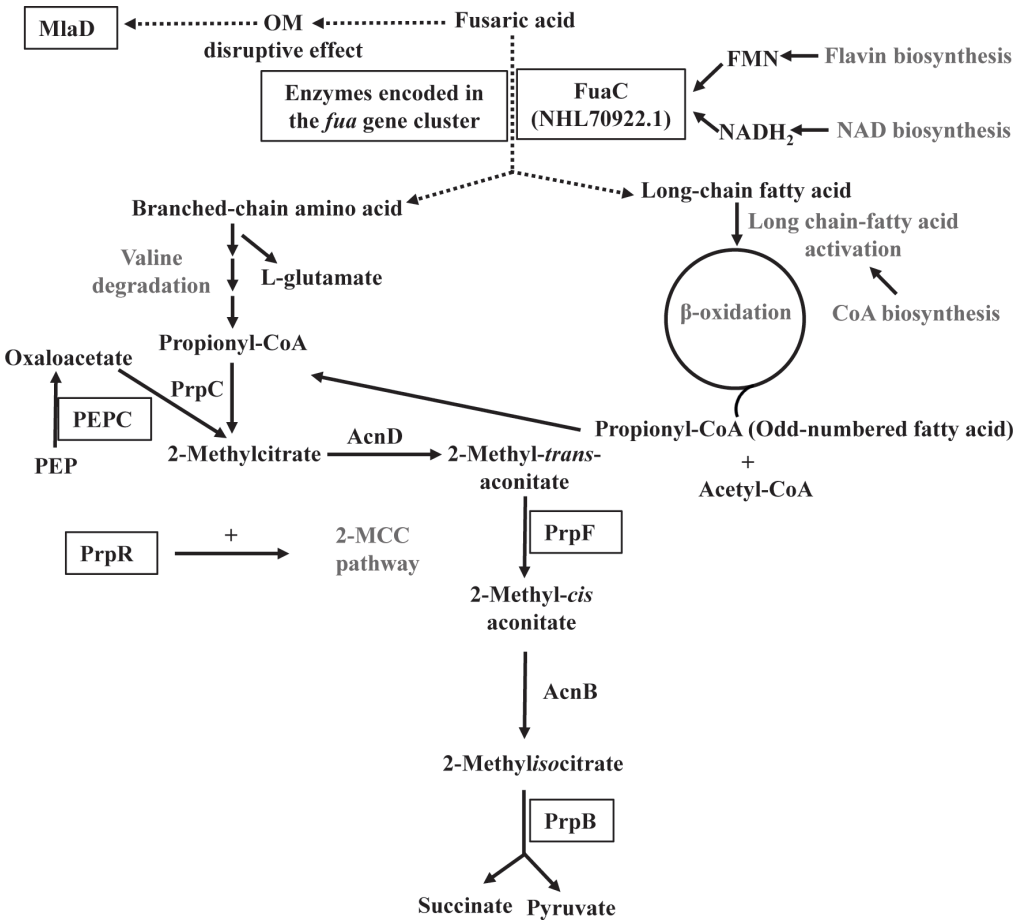

FIG 7 Schematic representation of key proteins and metabolic pathways likely required for fusaric acid catabolism in *B. ambifaria* T16. Proteins belonging to metabolic pathways written in gray were significantly more abundant during growth on fusaric acid compared to sodium citrate. Proteins essential for growth in the presence of fusaric acid are black-framed. OM, outer membrane; PEP, phosphoenolpyruvate.

is illustrated by the fact that Gram-positive species exhibit lower MIC values for this mycotoxin compared to Gram-negative species (19–21, 23).

The transposon insertion in the gene EIB72_16280 (*B. ambifaria* FA21), encoding a predicted acyl-CoA dehydrogenase (NHL67938.1), completely abolished the capability of *B. ambifaria* T16 to use FA as carbon and nitrogen source. However, the sensitivity to FA was not affected by this insertion, suggesting that this acyl-CoA dehydrogenase could be implicated in FA catabolism. The gene EIB72_16280 clusters with a gene encoding a LysR-type transcriptional regulator (NHL67939.1), two genes for short-chain dehydrogenases, a gene encoding an aminoglycoside phosphotransferase and a gene predicted to encode a protein belonging to the histidine phosphatase superfamily (NHL67935.1). It is noteworthy that the LysR regulator NHL6739.1 has a C-terminal substrate binding domain involved in the catabolism of nitroaromatic/naphthalene compounds (71).

The interruption of the 2-MCC genes *prpR*, *prpF*, and *prpB* (mutants *B. ambifaria* FA4, FA92, FA91, and FA2) completely abolished the capability of *B. ambifaria* T16 to grow with FA as the sole carbon and energy source. Moreover, these insertional mutants were also affected in the capability to use FA as sole nitrogen source, but to different extents. According to the proteomic analysis, all 2-MCC enzymes were significantly more abundant during growth with FA compared to CA. Altogether, these results indicated that the 2-methylcitrate pathway plays a very important function during the growth of *B. ambifaria* T16 on FA as carbon source (Fig. 7) . The role of the 2-MCC

in the detoxification of propionyl-CoA and its derived catabolites (e.g., 2-methylcitrate, 2-methyl*iso*citrate) has been extensively demonstrated in bacteria and fungi (59, 72–80). A non-functional 2-MCC causes severe growth inhibition when propionate is added to the growth medium. Propionyl-CoA can be generated by the activation of propionate or from the catabolism of different molecules, such as odd-chain fatty acids, branched-chain amino acids, or some aromatic compounds (81–84). The inability of the 2-MCC insertional mutants to grow with FA, led us to think that propionyl-CoA was generated during FA catabolism (Fig. 7). When the tolerance to FA was evaluated in these mutants, mutant *B. ambifaria* FA2 which possesses the mini-Tn*5* insertion in the gene encoding 2-methyl*iso*citrate lyase (2-MCL)-showed a very high sensitivity to FA. For the remaining 2-MCC mutants, the MIC values obtained were similar to that of the wild-type strain. In agreement with this observation, the loss of 2-MCL activity in *M. smegmatis* was more detrimental to growth on propionate than the absence of all 2-MCC enzymes (59). Moreover, Eoh and Rhee (75) have demonstrated that the extreme vulnerability of 2-MCL deficient strains during growth on propionate is due to several metabolic defects resulting from a truncated 2-MCC pathway. These defects include depletion of oxaloacetate from the TCA cycle and gluconeogenic pathways, as well as accumulation of 2-methyl*iso*citrate, a noncompetitive inhibitor of the enzyme fructose 1,6-bisphosphatase (80). Our results showed that the absence of the gene encoding 2-MCL in *B. ambifaria* T16 caused a high sensitivity to FA and the incapability to grow on propionate and FA as carbon sources. The higher sensitivity to FA of the insertional mutant FA2 compared to the Δ*prpB* strain could be attributed to polar effects on the expression of the genes located downstream *prpB* (*prpC*, *prp*F, or *acnD*) due to the mini-transposon insertion. The introduction of *prpB* from *B. ambifaria* T16 or a gene (*icl1*) encoding an enzyme of *M. smegmatis* with dual 2-MCL and *iso*citrate lyase activities into the Δ*prpB* mutant of *B. ambifaria*, increased the tolerance to FA and the ability to grow on FA as sole carbon source, confirming the essentiality of the 2-MCL activity for FA catabolism. Moreover, overexpression of *prpB* shortened the long lag phase observed for the wild type strain during growth on PA and FA, which reinforces the importance of 2-MCL activity for adaptation under these growth conditions. The lower growth rates obtained for the Δ*prpB* strain expressing the *icl1* gene in comparison with the wild-type strain could be attributed to the augmented *iso*citrate lyase levels, which competes with the enzyme *iso*citrate dehydrogenase (85).

Insertion of the mini-Tn*5* in the locus EIB72_11905, encoding PEPC, eliminated the capability to grow with FA as carbon source but did not alter the capability to use FA as nitrogen source. The essentiality of PEPC on FA catabolism could be explained considering our hypothesis that propionyl-CoA is generated during FA degradation, and taking into account that the role of PEPC is to replenish oxaloacetate. This compound is one of the substrates of the 2-methylcitrate synthase PrpC, the enzyme that catalyzes the condensation of propionyl-CoA to form 2-methylcitrate (Fig. 7).

The analysis of the proteomic results using the Pathway Tools Omics module (86) showed that several enzymes predicted to be involved in the generation of propionyl-CoA, including acyl-CoA synthetases and proteins involved in valine catabolism were upregulated during the growth on FA as carbon source. Besides, enzymes involved in fatty acid catabolism were also highly overexpressed in M9 + FA. Taking this into account, it is reasonable to assume that a long-chain fatty acid and a branched-chain amino acid would be generated as intermediates during FA catabolism (Fig. 7).

As it was mentioned in the Introduction, FA is toxic for most soil inhabiting microbes (19). According to a screening performed on soil-inhabiting bacteria, the ability to grow on FA as carbon and energy source was not a common characteristic in this environment (32). The enzymes that showed the greatest differences in their intracellular levels during cultivation of *B. ambifaria* T16 with FA compared with CA (NHL70920.1–70924. 1) are encoded in a gene cluster that we designate *fua*, due to its likely role in FA catabolism. Interestingly, the *fua* cluster is located in a genomic region that is highly variable in *Burkholderia* species, and it was predicted to be part of a genomic island (52).

As the cleavage of the pyridine ring would require the action of an oxygenase and as FMOs were found to be involved in the initial step in the biodegradation of different N-heterocyclic aromatic compounds (65–68), we hypothesize that the flavin-monooxygenase enzyme encoded by *fuaC*, is involved in the catabolism of FA in *B. ambifaria* T16. The strain *B. ambifaria* Δ*fuaC* (T800) was unable to grow with FA as the sole carbon and nitrogen source. Introduction of *fuaC* into T800 was able to restore growth, confirming that this gene is essential for FA catabolism. The sensitivity to FA was not affected by the absence of *fuaC*, suggesting that *B. ambifaria* T16 possesses mechanisms to cope with the toxic effects of FA, such as an OM disruptive effect and iron sequestration (23). Moreover, the proteomic analysis showed a marked upregulation of some enzymes involved in flavin biosynthesis during cultivation of *B. ambifaria* T16 with FA, which reinforces the hypothesis of the implication of flavin-dependent enzymes in the degradation of the mycotoxin (Fig. 7).

FA is a pyridine derivative, and although several environmental bacteria are able to degrade different pyridine-containing molecules, there is not much information about the enzymes that catalyze the first step in the catabolism of these compounds. The hydroxylation of the pyridine ring was proposed to be the key initial step involved in the metabolism of this N-heterocyclic compound (87–90). Multi-component molybdenum-containing monooxygenases and mono-component FAD-dependent monooxygenases were reported to catalyze this reaction (87–92). In 2018, Perchant et al. (68) found that the catabolism of *N*-methylnicotinate started by the pyridine ring cleavage by a two-component FMO from the LLM family. These enzymes were also shown to catalyze the initial ring-opening reaction of other *N*-heterocyclic compounds, such as uracil (65) and tetramethylpyrazine (67). More recently, Časaité et al. (66) demonstrated that the two-component LLM PyrA catalyzes the first step in the pyridine biodegradation pathway of *Arthrobacter* sp. 68b. As described in the Results section, the FuaC LLM from *B. ambifaria* T16 shares between 23% and 34% identity to others LLMs involved in the catabolism of different N-heterocyclic compounds. It is worth mentioning that members of the LLM family usually share low amino acid sequences identity (93).

In conclusion, we report the identification of genes involved in the biodegradation of the mycotoxin FA by the soil bacterium *B. ambifaria* T16. We were able to demonstrate that a functional 2-MCC is essential for growth on FA as carbon and energy source, suggesting that propionyl-CoA is an intermediate in FA catabolism. Moreover, a two-component FMO of unknown function, encoded in a genomic region predicted to be located in a genomic island, was shown to be fundamental to support the growth of *B. ambifaria* T16 with FA as sole nitrogen, carbon and energy source (Fig. 7). This enzyme is a good candidate to catalyze the pyridine ring-opening reaction during the biodegradation of FA.

ACKNOWLEDGMENTS

The authors thank Dr. Miguel Valvano for providing plasmids pGPI-SceI and pDAI-SceI, and Victor de Lorenzo for the gift of plasmid pJMT6. The authors are grateful to Dr. Mariana Piuri for *Mycobacterium smegmatis* mc^2 155.

This work was supported by the National Agency for Scientific Promotion, Technological Development and Innovation (AGENCIA I + D + i. Grants PICT-2017-1500 and PICT-2020-SERIEA-02598), the National Research Council (CONICET, PUE 0136 and PIP 0307), and the Alexander von Humboldt Foundation. P.I.N. received financial support from The Novo Nordisk Foundation through grants NNF20CC0035580, *LiFe* (NNF18OC0034818), and *TARGET* (NNF21OC0067996), the Danish Council for Independent Research (*SWEET*, DFF-Research Project 8021-00039B), and the European Union's Horizon 2020 Research and Innovation Program under grant agreement no. 814418 (*SinFonia*).

AUTHOR AFFILIATIONS

[1]Instituto de Investigaciones en Biociencias Agrícolas y Ambientales (INBA), CONICET-Universidad de Buenos Aires, Buenos Aires, Argentina
[2]Protein Analysis Unit, BioMedical Center (BMC), Ludwig-Maximilians-Universität München, Martinsried, Germany
[3]Faculty Biology, Microbiology, Ludwig-Maximilians-Universität München, Martinsried, Germany
[4]Novo Nordisk Foundation Center for Biosustainability, Technical University of Denmark, Kongens Lyngby, Denmark
[5]Instituto de Cálculo (IC), CONICET-Universidad de Buenos Aires, Buenos Aires, Argentina
[6]Departamento de Química Biológica, Facultad de Ciencias Exactas y Naturales, Universidad de Buenos Aires, Buenos Aires, Argentina

AUTHOR ORCIDs

Kirsten Jung http://orcid.org/0000-0003-0779-6841
Pablo I. Nikel http://orcid.org/0000-0002-9313-7481
Jimena A. Ruiz http://orcid.org/0000-0003-0908-096X

FUNDING

Funder	Grant(s)	Author(s)
MINCyT | Agencia Nacional de Promoción Científica y Tecnológica (ANPCyT)	PICT-2017-1500	Jimena A. Ruiz
MINCyT | Agencia Nacional de Promoción Científica y Tecnológica (ANPCyT)	PICT-2020-SERIEA-02598	Jimena A. Ruiz
Consejo Nacional de Investigaciones Científicas y Técnicas (CONICET)	PUE0136	Jimena A. Ruiz
Consejo Nacional de Investigaciones Científicas y Técnicas (CONICET)	PIP0307	Jimena A. Ruiz
Alexander von Humboldt-Stiftung (AvH)		Kirsten Jung Jimena A. Ruiz
Novo Nordisk Fonden (NNF)	NNF20CC0035580	Pablo I. Nikel
Novo Nordisk Fonden (NNF)	LiFe NNF18OC0034818	Pablo I. Nikel
Novo Nordisk Fonden (NNF)	TARGET NNF21OC0067996	Pablo I. Nikel
Danish Council for Independent Research	SWEET DFF-Research Project 8021-00039B	Pablo I. Nikel
EC | Horizon Europe | 創新的歐洲 | HORIZON EUROPE European Innovation Council (EIC)	No. 814418 SinFonia	Pablo I. Nikel

AUTHOR CONTRIBUTIONS

Matias Vinacour, Data curation, Formal analysis, Investigation, Methodology, Validation, Visualization, Writing – original draft | Mauro Moiana, Investigation | Ignasi Forné, Data curation, Formal analysis, Investigation, Methodology, Validation, Visualization, Writing – review and editing | Kirsten Jung, Conceptualization, Funding acquisition, Resources, Supervision, Writing – review and editing | Micaela Bertea, Investigation, Methodology | Patricia M. Calero Valdayo, Methodology | Pablo I. Nikel, Funding acquisition, Methodology, Resources, Supervision, Writing – review and editing | Axel Imhof, Funding acquisition, Methodology, Resources | Miranda C. Palumbo, Methodology, Resources, Supervision | Dario Fernández Do Porto, Funding acquisition, Resources, Supervision | Jimena A. Ruiz, Conceptualization, Data curation, Formal analysis, Funding acquisition,

Investigation, Methodology, Project administration, Resources, Supervision, Validation, Visualization, Writing – original draft

DATA AVAILABILITY

The data sets generated and analyzed during the current study are available from the corresponding author on reasonable request.

ADDITIONAL FILES

The following material is available online.

Supplemental Material

Table S1 and Fig. S1 to S3 (AEM00630-23-S0001.pdf). Proteomic data set and tolerance to outer membrane disruptive agents

REFERENCES

1. Bacon CW, Porter JK, Norred WP, Leslie JF. 1996. Production of fusaric acid by *Fusarium* species. Appl Environ Microbiol 62:4039–4043. https://doi.org/10.1128/aem.62.11.4039-4043.1996
2. Ma L-J, Geiser DM, Proctor RH, Rooney AP, O'Donnell K, Trail F, Gardiner DM, Manners JM, Kazan K. 2013. *Fusarium* pathogenomics. Annu Rev Microbiol 67:399–416. https://doi.org/10.1146/annurev-micro-092412-155650
3. Pegg GF. 1981. Biochemistry and physiology of pathogenesis, p 193–246. In Mace ME, AA Bell, CH Beckman (ed), Fungal wilt diseases of plants. Academic Press Inc, New York.
4. El-Hassan KI, El-Saman MG, Mosa AA, Mostafa M 2. 2007. Variation among *Fusarium* spp., the causal of potato tuber dry rot in their pathogenicity and mycotoxins production. Egypt J Phytopathol 35:53–68.
5. Liu S, Li J, Zhang Y, Liu N, Viljoen A, Mostert D, Zuo C, Hu C, Bi F, Gao H, Sheng O, Deng G, Yang Q, Dong T, Dou T, Yi G, Ma LJ, Li C 2. 2020. Fusaric acid Instigates the invasion of banana by Fusarium oxysporum f. sp. cubense TR4. New Phytol 225:913–929. https://doi.org/10.1111/nph.16193
6. Ding Z, Yang L, Wang G, Guo L, Liu L, Wang J, Huang J. 2018. Fusaric acid is a virulence factor of *Fusarium oxysporum* f.sp. *cubense* on banana plantlets. Trop plant pathol 43:297–305. https://doi.org/10.1007/s40858-018-0230-4
7. López-Díaz C, Rahjoo V, Sulyok M, Ghionna V, Martín-Vicente A, Capilla J, Di Pietro A, López-Berges MS. 2018. Fusaric acid contributes to virulence of *Fusarium oxysporum* on plant and mammalian hosts. Mol Plant Pathol 19:440–453. https://doi.org/10.1111/mpp.12536
8. Oubraim S, Sedra MH, Lazrek1HB. 2018. Fusaric acid and phytotoxic metabolites produced by *Fusarium oxysporum* f.sp. *albedinis*: effects on date palm and their use for resistance screening trial. J Mater Environ Sci 9:1622–1629. https://doi.org/10.26872/jmes.2018.9.5.180
9. Chakrabarti DK, Ghosal S 1. 1989. The disease cycle of mango malformation induced by *Fusarium moniliforme* var. subglutinans and the curative effects of mangiferinmetal chelates. Journal of Phytopathology 125:238–246. https://doi.org/10.1111/j.1439-0434.1989.tb01065.x
10. Singh VK, Upadhyay RS. 2014. Fusaric acid induced cell death and changes in oxidative metabolism of *Solanum lycopersicum L*. Bot Stud 55:66. https://doi.org/10.1186/s40529-014-0066-2
11. Singh VK, Singh HB, Upadhyay RS. 2017. Role of fusaric acid in the development of '*Fusarium* wilt symptoms in tomato: physiological, biochemical and proteomic perspectives. Plant Physiol Biochem 118:320–332. https://doi.org/10.1016/j.plaphy.2017.06.028
12. Pavlovkin J, Mistrík I, Prokop M. 2004. Some aspects of the phytotoxic action of fusaric acid on primary *Ricinus* roots. Plant Soil Environ 50:397–401. https://doi.org/10.17221/4050-PSE
13. Wang M, Ling N, Dong X, Liu X, Shen Q, Guo S 2. 2014. Effect of fusaric acid on the leaf physiology of cucumber seedlings. Eur J Plant Pathol 138:103–112. https://doi.org/10.1007/s10658-013-0306-4
14. Nurcahyani E, Sholekhah S, Qudus HI. 2021. Analysis of total carbohydrate and chlorophyll content of the orchid plantlet [*Phalaenopsis amabilis* (L.) Bl.] resistant *Fusarium* wilt disease. J Phys: Conf Ser 1751. https://doi.org/10.1088/1742-6596/1751/1/012061
15. Arie T. 2019. *Fusarium* diseases of cultivated plants, control, diagnosis, and molecular and genetic studies. J Pestic Sci 44:275–281. https://doi.org/10.1584/jpestics.J19-03
16. Fravel D, Olivain C, Alabouvette C. 2003. *Fusarium oxysporum* and its biocontrol. New Phytol 157:493–502. https://doi.org/10.1046/j.1469-8137.2003.00700.x
17. Yates IE, Arnold JW, Hinton DM, Basinger W, Walcott RR 2. 2003 *Fusarium verticillioides* induction of maize seed rot and its control. Can J Microbiol 81:422–428. https://doi.org/10.1139/b03-034
18. Dita M, Barquero M, Heck D, Mizubuti ESG, Staver CP. 2018. *Fusarium* wilt of banana: current knowledge on epidemiology and research needs toward sustainable disease management. Front Plant Sci 9:1468. https://doi.org/10.3389/fpls.2018.01468
19. Crutcher FK, Puckhaber LS, Stipanovic RD, Bell AA, Nichols RL, Lawrence KS, Liu J. 2017. Microbial resistance mechanisms to the antibiotic and phytotoxin fusaric acid. J Chem Ecol 43:996–1006. https://doi.org/10.1007/s10886-017-0889-x
20. Bacon CW, Hinton DM, Hinton A. 2006. Growth-inhibiting effects of concentrations of fusaric acid on the growth of *Bacillus mojavensis* and other biocontrol *Bacillus* species. J Appl Microbiol 100:185–194. https://doi.org/10.1111/j.1365-2672.2005.02770.x
21. Landa BB, Cachinero-Díaz JM, Lemanceau P, Jiménez-Díaz RM, Alabouvette C. 2002. Effect of fusaric acid and phytoanticipins on growth of rhizobacteria and *Fusarium oxysporum*. Can J Microbiol 48:971–985. https://doi.org/10.1139/w02-094
22. Sao Emani C, Williams MJ, Wiid IJ, Baker B, Carolis C. 2018. Compounds with potential activity against *Mycobacterium tuberculosis*. Antimicrob Agents Chemother 62:e02236-17. https://doi.org/10.1128/AAC.02236-17
23. Ruiz JA, Bernar EM, Jung K. 2015. Production of siderophores increases resistance to fusaric acid in *Pseudomonas protegens* Pf-5. PLoS One 10:e0117040. https://doi.org/10.1371/journal.pone.0117040
24. Duffy BK, Keel C, Défago G 2. 2004. Potential role of pathogen signaling in multitrophic plant-microbe interactions involved in disease protection. Appl Environ Microbiol 70:1836–1842. https://doi.org/10.1128/AEM.70.3.1836-1842.2004
25. Notz R, Maurhofer M, Dubach H, Haas D, Défago G. 2002. Fusaric acid-producing strains of *Fusarium oxysporum* alter 2,4-diacetylphloroglucinol biosynthetic gene expression in *Pseudomonas fluorescens* CHA0 *in vitro* and in the rhizosphere of wheat. Appl Environ Microbiol 68:2229–2235. https://doi.org/10.1128/AEM.68.5.2229-2235.2002
26. Quecine MC, Kidarsa TA, Goebel NC, Shaffer BT, Henkels MD, Zabriskie TM, Loper JE. 2015. An interspecies signaling system mediated by fusaric acid has parallel effects on antifungal metabolite production by *Pseudomonas protegens* strain Pf-5 and antibiosis of *Fusarium* spp. Appl Environ Microbiol 82:1372–1382. https://doi.org/10.1128/AEM.02574-15

27. van Rij ET, Girard G, Lugtenberg BJJ, Bloemberg GV. 2005. Influence of fusaric acid on phenazine-1-carboxamide synthesis and gene expression of *Pseudomonas chlororaphis* strain PCL1391. Microbiology 151:2805–2814. https://doi.org/10.1099/mic.0.28063-0
28. Venkatesh N, Keller NP. 2019. Mycotoxins in conversation with bacteria and fungi. Front Microbiol 10:403. https://doi.org/10.3389/fmicb.2019.00403
29. Crutcher FK, Liu J, Puckhaber LS, Stipanovic RD, Duke SE, Bell AA, Williams HJ, Nichols RL. 2014. Conversion of fusaric acid to fusarinol by *Aspergillus tubingensis*: a detoxification reaction. J Chem Ecol 40:84–89. https://doi.org/10.1007/s10886-013-0370-4
30. Crutcher FK, Puckhaber LS, Bell AA, Liu J, Duke SE, Stipanovic RD, Nichols RL. 2017. Detoxification of fusaric acid by the soil microbe *Mucor rouxii*. J Agric Food Chem 65:4989–4992. https://doi.org/10.1021/acs.jafc.7b01655
31. Fakhouri W, Walker F, Armbruster W, Buchenauer H. 2003. Detoxification of fusaric acid by a nonpathogenic *Colletotrichum* sp. Physiological and Molecular Plant Pathology 63:263–269. https://doi.org/10.1016/j.pmpp.2004.03.004
32. Simonetti E, Roberts IN, Montecchia MS, Gutierrez-Boem FH, Gomez FM, Ruiz JA. 2018. A novel *Burkholderia ambifaria* strain able to degrade the mycotoxin fusaric acid and to inhibit *Fusarium* spp. growth. Microbiol Res 206:50–59. https://doi.org/10.1016/j.micres.2017.09.008
33. Miller JH. 1972. Experiments in molecular genetics. Cold Spring Harbor Laboratory Press, Cold Spring Harbor. NY.
34. Lageveen RG, Huisman GW, Preusting H, Ketelaar P, Eggink G, Witholt B. 1988. Formation of polyesters by *Pseudomonas oleovorans*: effect of substrates on formation and composition of poly-(R)-3-hydroxyalkanoates and poly-(R)-3-hydroxyalkenoates. Appl Environ Microbiol 54:2924–2932. https://doi.org/10.1128/aem.54.12.2924-2932.1988
35. Herrero M, de Lorenzo V, Timmis KN. 1990. Transposon vectors containing non-antibiotic resistance selection markers for cloning and stable chromosomal insertion of foreign genes in gram-negative bacteria. J Bacteriol 172:6557–6567. https://doi.org/10.1128/jb.172.11.6557-6567.1990
36. Miller VL, Mekalanos J 1. 1988. A novel suicide vector and its use in construction of insertion mutations: osmoregulation of outer membrane proteins and virulence determinants in *Vibrio cholerae* requires *tox*R. J Bacteriol 170:2575–2583. https://doi.org/10.1128/jb.170.6.2575-2583.1988
37. Snapper SB, Melton RE, Mustafa S, Kieser T, Jacobs WR. 1990. Isolation and characterization of efficient plasmid transformation mutants of *Mycobacterium smegmatis*. Mol Microbiol 4:1911–1919. https://doi.org/10.1111/j.1365-2958.1990.tb02040.x
38. Fernández-Tresguerres ME, Martín M, García de Viedma D, Giraldo R, Díaz-Orejas R. 1995. Host growth temperature and a conservative amino acid substitution in the replication protein of pPS10 influence plasmid host range. J Bacteriol 177:4377–4384. https://doi.org/10.1128/jb.177.15.4377-4384.1995
39. Sanchez-Romero JM, Diaz-Orejas R, De Lorenzo V. 1998. Resistance to tellurite as a selection marker for genetic manipulations of *Pseudomonas strains*. Appl Environ Microbiol 64:4040–4046. https://doi.org/10.1128/AEM.64.10.4040-4046.1998
40. Silva-Rocha R, Martínez-García E, Calles B, Chavarría M, Arce-Rodríguez A, de Las Heras A, Páez-Espino AD, Durante-Rodríguez G, Kim J, Nikel PI, Platero R, de Lorenzo V. 2013. The standard European vector architecture (SEVA): a coherent platform for the analysis and deployment of complex prokaryotic phenotypes. Nucleic Acids Res 41:D666–75. https://doi.org/10.1093/nar/gks1119
41. Flannagan RS, Linn T, Valvano MA. 2008. A system for the construction of targeted unmarked gene deletions in the genus *Burkholderia*. Environ Microbiol 10:1652–1660. https://doi.org/10.1111/j.1462-2920.2008.01576.x
42. Das S, Noe JC, Paik S, Kitten T. 2005. An improved arbitrary primed PCR method for rapid characterization of transposon insertion sites. J Microbiol Methods 63:89–94. https://doi.org/10.1016/j.mimet.2005.02.011
43. Martínez-García E, Calles B, Arévalo-Rodríguez M, de Lorenzo V. 2011. PBAM1: an all-synthetic genetic tool for analysis and construction of complex bacterial phenotypes. BMC Microbiol 11:38. https://doi.org/10.1186/1471-2180-11-38
44. Simonetti E, Alvarez F, Feldman N, Vinacour M, Roberts IN, Ruiz JA. 2021. Genomic insights into the potent antifungal activity of *B. ambifaria* T16. Biological Control 155:104530. https://doi.org/10.1016/j.biocontrol.2020.104530
45. Ausubel FM, Brent R, Kingston R, Moore DD, Seiman J, Smith JA, Struhl K. 1987. Current protocols in molecular biology. John Wiley & Sons, New York.
46. Martínez-García E, Fraile S, Algar E, Aparicio T, Velázquez E, Calles B, Tas H, Blázquez B, Martín B, Prieto C, Sánchez-Sampedro L, Nørholm MHH, Volke DC, Wirth NT, Dvořák P, Alejaldre L, Grozinger L, Crowther M, Goñi-Moreno A, Nikel PI, Nogales J, de Lorenzo V. 2023. SEVA 4.0: an update of the standard European vector architecture database for advanced analysis and programming of bacterial phenotypes. Nucleic Acids Res 51:D1558–D1567. https://doi.org/10.1093/nar/gkac1059
47. Cavaleiro AM, Kim SH, Seppälä S, Nielsen MT, Nørholm MHH. 2015. Accurate DNA assembly and genome engineering with optimized uracil excision cloning. ACS Synth Biol 4:1042–1046. https://doi.org/10.1021/acssynbio.5b00113
48. Hilgarth RS, Lanigan TM. 2020. Optimization of overlap extension PCR for efficient transgene construction. MethodsX 7:100759. https://doi.org/10.1016/j.mex.2019.12.001
49. Martínez-García E, de Lorenzo V. 2011. Engineering multiple genomic deletions in gram-negative bacteria: analysis of the multi-resistant antibiotic profile of *Pseudomonas putida* KT2440. Environ Microbiol 13:2702–2716. https://doi.org/10.1111/j.1462-2920.2011.02538.x
50. Gasperotti A, Göing S, Fajardo-Ruiz E, Forné I, Jung K. 2020. Function and regulation of the pyruvate transporter CstA in *Escherichia coli*. Int J Mol Sci 21:9068. https://doi.org/10.3390/ijms21239068
51. Tyanova S, Temu T, Sinitcyn P, Carlson A, Hein MY, Geiger T, Mann M, Cox J. 2016. The Perseus computational platform for comprehensive analysis of (prote)omics data. Nat Methods 13:731–740. https://doi.org/10.1038/nmeth.3901
52. Alvarez F, Simonetti E, Draghi WO, Vinacour M, Palumbo MC, Do Porto DF, Montecchia MS, Roberts IN, Ruiz JA. 2022. Genome mining of *Burkholderia ambifaria* strain T16, a rhizobacterium able to produce antimicrobial compounds and degrade the mycotoxin fusaric acid. World J Microbiol Biotechnol 38:114. https://doi.org/10.1007/s11274-022-03299-0
53. Paley S, Parker K, Spaulding A, Tomb J-F, O'Maille P, Karp PD. 2017. The omics dashboard for interactive exploration of gene-expression data. Nucleic Acids Res 45:12113–12124. https://doi.org/10.1093/nar/gkx910
54. Suvorova IA, Ravcheev DA, Gelfand MS. 2012. Regulation and evolution of malonate and propionate catabolism in proteobacteria. J Bacteriol 194:3234–3240. https://doi.org/10.1128/JB.00163-12
55. WilkeA, ZagnitkoO. 2008. The RAST server: rapid annotations using subsystems technology. BMC Genomics 9:75. https://doi.org/10.1186/1471-2164-9-75
56. Malinverni JC, Silhavy TJ. 2009. An ABC transport system that maintains lipid asymmetry in the gram-negative outer membrane. Proc Natl Acad Sci U S A 106:8009–8014. https://doi.org/10.1073/pnas.0903229106
57. Deutscher MP. 2009. Maturation and degradation of ribosomal RNA in bacteria. Prog Mol Biol Transl Sci 85:369–391. https://doi.org/10.1016/S0079-6603(08)00809-X
58. Del Campo M, Kaya Y, Ofengand J. 2001. Identification and site of action of the remaining four putative pseudouridine synthases in *Escherichia coli*. RNA 7:1603–1615.
59. Upton AM, McKinney JD. 2007. Role of the methylcitrate cycle in propionate metabolism and detoxification in *Mycobacterium smegmatis*. Microbiology153:3973–3982. https://doi.org/10.1099/mic.0.2007/011726-0
60. Ogasawara H, Ohe S, Ishihama A. 2015. Role of transcription factor NimR (YeaM) in sensitivity control of *Escherichia coli* to 2-nitroimidazole. FEMS Microbiol Lett 362:1–8. https://doi.org/10.1093/femsle/fnu013
61. Teufel R, Mascaraque V, Ismail W, Voss M, Perera J, Eisenreich W, Haehnel W, Fuchs G. 2010. Bacterial phenylalanine and phenylacetate catabolic pathway revealed. Proc Natl Acad Sci U S A 107:14390–14395. https://doi.org/10.1073/pnas.1005399107
62. Bruender NA, Bandarian V. 2017. The creatininase homolog MftE from *Mycobacterium smegmatis* catalyzes a peptide cleavage reaction in the biosynthesis of a novel ribosomally synthesized post-translationally

modified peptide (RiPP). J Biol Chem 292:4371–4381. https://doi.org/10.1074/jbc.M116.762062
63. Tsuru D, Oka I, Yoshimoto T 1. 1976. Creatinine decomposing enzymes in *Pseudomonas putida*. Agric Biol Chem 40:1011–1018. https://doi.org/10.1271/bbb1961.40.1011
64. Huijbers MME, Montersino S, Westphal AH, Tischler D, van Berkel WJH. 2014. Flavin dependent monooxygenases. Arch Biochem Biophys 544:2–17. https://doi.org/10.1016/j.abb.2013.12.005
65. Mukherjee T, Zhang Y, Abdelwahed S, Ealick SE, Begley TP. 2010. Catalysis of a flavoenzyme-mediated amide hydrolysis. J Am Chem Soc 132:5550–5551. https://doi.org/10.1021/ja9107676
66. Časaitė V, Stanislauskienė R, Vaitekūnas J, Tauraitė D, Rutkienė R, Gasparavičiūtė R, Meškys R. 2020. Microbial degradation of pyridine: a complete pathway in *Arthrobacter* sp. strain 68b deciphered. Appl Environ Microbiol 86:e00902-20. https://doi.org/10.1128/AEM.00902-20
67. Kutanovas S, Stankeviciute J, Urbelis G, Tauraite D, Rutkiene R, Meskys R. 2013. Identification and characterization of a tetramethylpyrazine catabolic pathway in *Rhodococcus jostii* TMP1. Appl Environ Microbiol 79:3649–3657. https://doi.org/10.1128/AEM.00011-13
68. Perchat N, Saaidi P-L, Darii E, Pellé C, Petit J-L, Besnard-Gonnet M, de Berardinis V, Dupont M, Gimbernat A, Salanoubat M, Fischer C, Perret A. 2018. Elucidation of the trigonelline degradation pathway reveals previously undescribed enzymes and metabolites. Proc Natl Acad Sci U S A 115:E4358–E4367. https://doi.org/10.1073/pnas.1722368115
69. Kim K, Lee S, Lee K, Lim D. 1998. Isolation and characterization of toluene-sensitive mutants from the toluene-resistant bacterium *Pseudomonas putida* GM73. J Bacteriol 180:3692–3696. https://doi.org/10.1128/JB.180.14.3692-3696.1998
70. Bernier SP, Son S, Surette MG. 2018. The MLA pathway plays an essential role in the intrinsic resistance of *Burkholderia cepacia* complex species to antimicrobials and host innate components. J Bacteriol 200:e00156-18. https://doi.org/10.1128/JB.00156-18
71. Lu S, Wang J, Chitsaz F, Derbyshire MK, Geer RC, Gonzales NR, Gwadz M, Hurwitz DI, Marchler GH, Song JS, Thanki N, Yamashita RA, Yang M, Zhang D, Zheng C, Lanczycki CJ, Marchler-Bauer A. 2020. CDD/SPARCLE: the conserved domain database in 2020. Nucleic Acids Res 48:D265–D268. https://doi.org/10.1093/nar/gkz991
72. Brock M. 2005. Generation and phenotypic characterization of *Aspergillus nidulans* methylisocitrate lyase deletion mutants: methylisocitrate inhibits growth and conidiation. Appl Environ Microbiol 71:5465–5475. https://doi.org/10.1128/AEM.71.9.5465-5475.2005
73. Brock M, Buckel W 2. n.d. On the mechanism of action of the antifungal agent propionate propionyl-CoA inhibits glucose metabolism in *Aspergillus nidulans*. Eur J Biochem 271:3227–3241. https://doi.org/10.1111/j.1432-1033.2004.04255.x
74. Brock M, Fischer R, Linder D, Buckel W. 2000. Methylcitrate synthase from *Aspergillus nidulans*: implications for propionate as an antifungal agent. Mol Microbiol 35:961–973. https://doi.org/10.1046/j.1365-2958.2000.01737.x
75. Eoh H, Rhee KY. 2014. Methylcitrate cycle defines the bactericidal essentiality of isocitrate lyase for survival of *Mycobacterium tuberculosis* on fatty acids. Proc Natl Acad Sci U S A 111:4976–4981. https://doi.org/10.1073/pnas.1400390111
76. Horswill AR, Dudding AR, Escalante-Semerena JC. 2001. Studies of propionate toxicity in *Salmonella enterica* identify 2-methylcitrate as a potent inhibitor of cell growth. J Biol Chem 276:19094–19101. https://doi.org/10.1074/jbc.M100244200
77. Lee JJ, Lim J, Gao S, Lawson CP, Odell M, Raheem S, Woo J, Kang SH, Kang SS, Jeon BY, Eoh H. 2018. Glutamate mediated metabolic neutralization mitigates propionate toxicity in intracellular *Mycobacterium tuberculosis*. Sci Rep 8:8506. https://doi.org/10.1038/s41598-018-26950-z
78. Maruyama K, Kitamura H. 1985. Mechanisms of growth inhibition by propionate and restoration of the growth by sodium bicarbonate or acetate in *Rhodopseudomonas sphaeroides* S. J Biochem 98:819–824. https://doi.org/10.1093/oxfordjournals.jbchem.a135340
79. Plassmeier J, Barsch A, Persicke M, Niehaus K, Kalinowski J. 2007. Investigation of central carbon metabolism and the 2-methylcitrate cycle in *Corynebacterium glutamicum* by metabolic profiling using gas chromatography-mass spectrometry. J Biotechnol 130:354–363. https://doi.org/10.1016/j.jbiotec.2007.04.026
80. Rocco CJ, Escalante-Semerena JC. 2010. In *Salmonella enterica*, 2-methylcitrate blocks gluconeogenesis. J Bacteriol 192:771–778. https://doi.org/10.1128/JB.01301-09
81. Johnson GR, Jain RK, Spain JC. 2000. Properties of the trihydroxytoluene oxygenase from *Burkholderia cepacia* R34: an extradiol dioxygenase from the 2,4-dinitrotoluene pathway. Arch Microbiol 173:86–90. https://doi.org/10.1007/s002039900111
82. Nazarova EV, Montague CR, La T, Wilburn KM, Sukumar N, Lee W, Caldwell S, Russell DG, VanderVen BC. 2017. Rv3723/LucA coordinates fatty acid and cholesterol uptake in *Mycobacterium tuberculosis*. Elife 6:e26969. https://doi.org/10.7554/eLife.26969
83. Suen WC, Spain JC. 1993. Cloning and characterization of *Pseudomonas* sp. strain DNT genes for 2,4-dinitrotoluene degradation. J Bacteriol 175:1831–1837. https://doi.org/10.1128/jb.175.6.1831-1837.1993
84. Zhang Y-Q, Brock M, Keller NP. 2004. Connection of Propionyl-CoA metabolism to polyketide biosynthesis in *Aspergillus nidulans*. Genetics 168:785–794. https://doi.org/10.1534/genetics.104.027540
85. Cozzone AJ. 1998. Regulation of acetate metabolism by protein phosphorylation in enteric bacteria. Annu Rev Microbiol 52:127–164. https://doi.org/10.1146/annurev.micro.52.1.127
86. Karp PD, Midford PE, Billington R, Kothari A, Krummenacker M, Latendresse M, Ong WK, Subhraveti P, Caspi R, Fulcher C, Keseler IM, Paley SM. 2021. Pathway tools version 23.0 update: software for pathway/genome informatics and systems biology. Brief Bioinform 22:109–126. https://doi.org/10.1093/bib/bbz104
87. Jiménez JI, Canales A, Jiménez-Barbero J, Ginalski K, Rychlewski L, García JL, Díaz E. 2008. Deciphering the genetic determinants for aerobic nicotinic acid degradation: the NIC cluster from *Pseudomonas putida* KT2440. Proc Natl Acad Sci U S A 105:11329–11334. https://doi.org/10.1073/pnas.0802273105
88. Li H, Xie K, Yu W, Hu L, Huang H, Xie H, Wang S, Löffler FE. 2016. Nicotine dehydrogenase complexed with 6-hydroxypseudooxynicotine oxidase involved in the hybrid nicotine-degrading pathway in *Agrobacterium tumefaciens* S33. Appl Environ Microbiol 82:1745–1755. https://doi.org/10.1128/AEM.03909-15
89. Qiu J, Liu B, Zhao L, Zhang Y, Cheng D, Yan X, Jiang J, Hong Q, He J, Kivisaar M. 2018. A novel degradation mechanism for pyridine derivatives in *Alcaligenes faecalis* JQ135. Appl Environ Microbiol 84:e00910-18. https://doi.org/10.1128/AEM.00910-18
90. Yu H, Tang H, Li Y, Xu P, Kivisaar M. 2015. Molybdenum-containing nicotine hydroxylase genes in a nicotine degradation pathway that is a variant of the pyridine and pyrrolidine pathways. Appl Environ Microbiol 81:8330–8338. https://doi.org/10.1128/AEM.02253-15
91. Qiu J, Zhao L, Xu S, Chen Q, Chen L, Liu B, Hong Q, Lu Z, He J. 2019. Identification and characterization of a novel *pic* gene cluster responsible for picolinic acid degradation in *Alcaligenes faecalis* JQ135. J Bacteriol 201:e00077-19. https://doi.org/10.1128/JB.00077-19
92. Yu H, Hausinger RP, Tang H-Z, Xu P. 2014. Mechanism of the 6-hydroxy-3-succinoyl-pyridine 3-monooxygenase flavoprotein from *Pseudomonas putida* S16. J Biol Chem 289:29158–29170. https://doi.org/10.1074/jbc.M114.558049
93. Ellis HR. 2010. The FMN-dependent two-component monooxygenase systems. Arch Biochem Biophys 497:1–12. https://doi.org/10.1016/j.abb.2010.02.007